

Transmission phase lapses in quantum dots: the role of dot-lead coupling asymmetry

D I Golosov¹ and Yuval Gefen²

¹ Racah Institute of Physics, the Hebrew University, Jerusalem 91904, Israel

E-mail: golosov@phys.huji.ac.il

² Dept. of Condensed Matter Physics, Weizmann Institute of Science, Rehovot 76100, Israel

E-mail: yuval.gefen@weizmann.ac.il

Abstract. Lapses of transmission phase in transport through quantum dots are ubiquitous already in the absence of interaction, in which case their precise location is determined by the signs and magnitudes of the tunnelling matrix elements. However, actual measurements for a quantum dot embedded in an Aharonov-Bohm interferometer show systematic sequences of phase lapses separated by Coulomb peaks – an issue that attracted much attention and generated controversy. Using a two-level quantum dot as an example we show that this phenomenon can be accounted for by the combined effect of asymmetric dot-lead couplings (left lead/right lead asymmetry as well as different level broadening for different levels) and interaction-induced "population switching" of the levels, rendering this behaviour generic. We construct and analyse a mean field scheme for an interacting quantum dot, and investigate the properties of the mean field solution, paying special attention to the character of its dependence (continuous vs. discontinuous) on the chemical potential or gate voltage.

PACS numbers: 73.21.La, 73.63.Kv, 73.23.Hk, 03.65.Vf

Submitted to: *New J. Phys.*

1. Introduction

Recent systematic studies [1, 2, 3] of current transmission through quantum dot (QD) embedded into an arm of an Aharonov–Bohm interferometer [4, 5, 6, 7], uncovered an unusual, correlated behaviour of transmission phase as a function of the gate voltage. Namely, between any two consecutive Coulomb blockade peaks the transmission phase suffers one abrupt change (phase lapse) of $-\pi$.

This surprising feature cannot be understood within the framework of a non-interacting QD model [8, 9, 10, 11], where the presence or absence of a phase lapse between the two transmission peaks is determined by the relative signs of the tunnelling matrix elements coupling the corresponding QD levels to the leads. Roughly speaking, two adjacent peaks are separated by a phase lapse as long as the product of the four matrix elements, coupling each of the two levels to the two leads, is positive [9, 10, 11]. Since experimentally there is no way to control these signs in a typical QD [12], this would suggest an approximately 50% probability of the presence of a phase lapse between the two consecutive peaks, in disagreement with experimental data. This dictates that the Coulomb (charging) interaction between electrons in the QD must be accounted for at some level [6, 13, 14, 15, 16].

Earlier investigations [15, 17] of the interaction effects in QDs resulted in the notion of “population switching” between the broad (strongly coupled to the leads) and narrow dot levels with varying gate voltage (or equivalently, with varying chemical potential). This phenomenon, which subsequently attracted attention of both theorists [18, 19, 20, 21, 22, 23, 24, 25] and experimentalists (see, *e.g.*, reference [26]), consists in the narrow levels being shifted upward due to the Coulomb potential of electrons accumulated at a broad level, which remains near the Fermi energy (“hovers”) over an extended range of the gate voltage/chemical potential values. Within the latter range, successive narrow levels from time to time get rapidly filled with electrons (thereby emptying the broad level, hence the term “population switching” [15, 16, 17, 18]) and shift downward below the Fermi level. Available results [17, 27, 28] suggest that this switching may be either continuous or discontinuous, although no systematic study of the two scenarios has been performed. We note that already in references [27, 28] mean field approach (self-consistent Hartree approximation) has been employed. Apart from reference [17], where a QD with only one lead was considered, these early studies were all concerned with models where the absolute values of the tunnelling coupling of each individual level to the right and left lead were the same (“left-right symmetry”).

It is probably due to the latter circumstance that for a long time no attention has been paid to another generic interaction-induced mechanism which affects both the energy level structure and the transmission phase behaviour in an interacting QD. This mechanism, which is not effective in the opposite-sign left-right symmetric-coupling case *only*, in the context of more conventional solid state physics corresponds to forming excitonic correlations between different bands [29]. Within the mean-field approach to interacting QDs [30], a similar scenario consists in forming the off-diagonal average

values between the QD states, leading to interaction-induced hybridisation between the dot energy levels. We note that the importance of considering the generic, right-left asymmetric dot-lead coupling values was pointed out independently in reference [20].

For the case of a strongly-interacting QD in the Coulomb blockade regime one finds that even a small right-left asymmetry typically results in a large effective hybridisation (again in analogy with conventional impurity problems [29]), leading in turn to a change of the coupling sign for the effective dot levels (“minus” changed to “plus”), and to a presence of phase lapse between the two transmission peaks. These findings, reported earlier in reference [30], are in line with recent functional renormalisation group results obtained for both two-level [20, 21, 22] and multi-level [21] interacting dots. We also note the recent perturbative treatment [23] and treatments based on the renormalisation group/Bethe *ansatz* approach [24, 25].

In the present article, we investigate transmission through a QD in the spinless case at zero temperature. We begin by describing the behaviour of transmission phase for multi-level non-interacting dot in section 2. The mean-field approach to an interacting two-level QD is formulated in section 3. The remainder of the paper is devoted to illustrating and discussing *the two mechanisms, whose interplay brings about the abrupt changes of the transmission phase (as a function of the gate voltage or chemical potential) between the Coulomb blockade peaks*. First, in section 4 we discuss the “excitonic” restructuring of the QD spectrum, operational in the presence of a right-left asymmetry. Second, in section 5 we address the two scenarios (continuous and discontinuous) of “population switching” in the right-left symmetric case. The interplay between the two mechanisms is briefly described in section 6. The overall conclusions, along with some remarks on the generality of our results and a summary of outstanding questions, are relegated to section 7.

2. Phase Lapses in the Non-Interacting Case

Transmission phase lapses in a multilevel dot in the absence of electron-electron interaction. Dependence on the dot-lead coupling strength. The role of dot-lead coupling signs. General expression for the transmission amplitude. Example: a four-level dot.

In the present section, we discuss the behaviour of transmission phase in the case of a generic multi-level QD, in the absence of electron-electron interactions [9, 10, 11, 13, 14]. While our analysis here is far from being comprehensive, it allows to draw three important conclusions:

(i) Phase lapses represent a generic property of transmission through QDs. In other words, the transmission amplitude t_{tr} vanishing at certain values of the chemical potential or the gate voltage (at which point [10, 14] the value of the transmission phase jumps by $-\pi$) does not impose any restrictive condition on the QD parameters. We quote reference [30] for an analysis of what is often perceived as a contradiction between this statement and the Friedel sum rule.

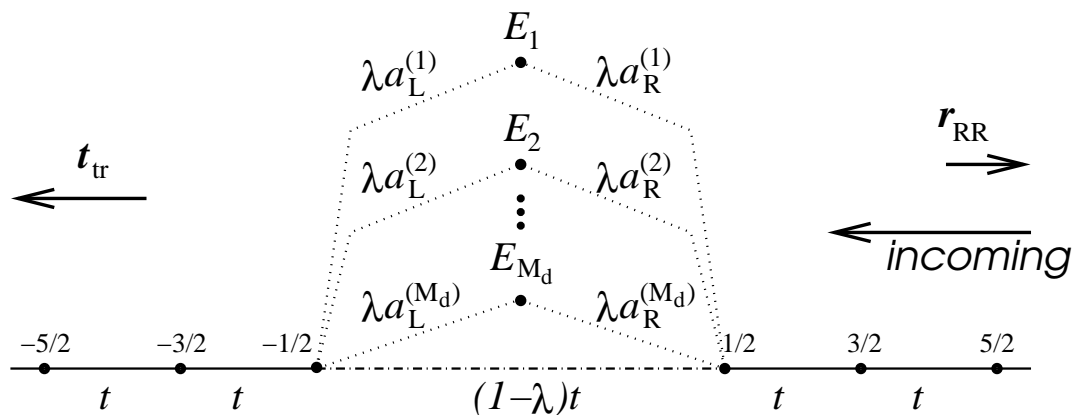


Figure 1. The model system, composed of a wire (chain) and a two-level dot, equations (2–5). Fully coupled dot corresponds to $\lambda = 1$. The arrows show incoming and outgoing waves, cf. equation (6)

(ii) As mentioned in the Introduction, in the non-interacting case the location of phase lapses with respect to transmission peaks is crucially affected by the relative signs of tunnelling matrix elements coupling the QD levels to the right and left leads [10, 9]. In particular, a necessary (but possibly not always sufficient) condition for a single phase lapse to occur between the two successive dot levels (corresponding to the two successive transmission peaks) is that the product of the tunnelling matrix elements coupling the two corresponding levels to the two leads is negative (we stress that this can be severely modified in the presence of electron-electron interactions and an asymmetric QD-lead coupling, see sections 4 and 5 below).

(iii) Beyond the above conclusion, the actual distribution of transmission zeroes with respect to the dot levels strongly depends on the values of the QD parameters, and this dependence can be rather complex.

Other analyses of the transmission phase in the absence of interaction [8] have demonstrated that disorder or geometry alone would not give rise to sequences of correlated inter-resonance phase lapses. The latter may however result from a presence of a very broad dot level [31].

The Hamiltonian of a generic non-interacting dot with M_d levels E_i (see figure 1) is given by

$$\mathcal{H}_d = \sum_{i=1}^{M_d} (E_i - \mu) \hat{d}_i^\dagger \hat{d}_i. \quad (1)$$

The dot is coupled to a one-dimensional wire

$$\mathcal{H}_w = -\frac{t}{2} \sum_j (\hat{c}_j^\dagger \hat{c}_{j+1} + \hat{c}_{j+1}^\dagger \hat{c}_j) - \mu \sum_j \hat{c}_j^\dagger \hat{c}_j, \quad (2)$$

(where t is half bandwidth and the half-integer index j labels the sites in the wire), by the perturbation V ,

$$V = V_T + \frac{t}{2} (\hat{c}_{1/2}^\dagger \hat{c}_{-1/2} + \hat{c}_{-1/2}^\dagger \hat{c}_{1/2}), \quad (3)$$

$$V_T = -\frac{1}{2} \sum_{i=1}^{M_d} \tilde{d}_j^\dagger \left(a_L^{(i)} \hat{c}_{-1/2} + a_R^{(i)} c_{1/2} \right) + \text{H.c.}, \quad (4)$$

where $a_L^{(i)}$ ($a_R^{(i)}$) are the real tunnelling elements coupling the i th dot level to the left (right) lead; these are assumed to be small in comparison to the bandwidth in the wire, $2t$. The second term on the r. h. s. in equation (3) corresponds to cutting the link between sites $j = -1/2$ and $j = 1/2$ of the wire. It is instructive to consider the system with varying perturbation strength, λ ,

$$\mathcal{H}_\lambda = \mathcal{H}_d + \mathcal{H}_w + \lambda V \quad (5)$$

(figure 1). While for $\lambda = 1$ this corresponds to a fully coupled dot (no direct hopping between right and left leads), characterised by a certain sequence of transmission peaks and transmission phase lapses, at $\lambda \rightarrow 0$ one recovers a featureless transmission amplitude, $t_{tr}(\mu) \equiv 1$ (hence $\Theta_{tr} \equiv 0$), of the decoupled case (unperturbed wire). As λ increases from 0 to 1, the profile of $\Theta_{tr}(\mu)$ evolves between these two limiting cases.

When searching for an eigenfunction ψ which away from the dot has the form of a left-moving, partially reflected wave,

$$\psi(x) = \begin{cases} t_{tr} \exp(-ikx), & x \leq -1/2, \\ \exp(-ikx) + r_{RR} \exp(ikx), & x \geq 1/2, \end{cases} \quad (6)$$

(where t_{tr} and r_{RR} are transmission and right-right reflection amplitudes respectively) one has to solve a system of $M_d + 2$ linear equations for the quantities $1/t_{tr}$, r_{RR}/t_{tr} , and the values ψ_i , $i = 1, \dots, M_d$ of the wave function on the dot levels (these correspond to the Schrödinger equation $\mathcal{H}_\lambda \psi = -t\psi \cos k$ written for the wire sites $j = \pm 1/2$ and for the dot levels). Zeroes of the transmission coefficient t_{tr} (at $\lambda \neq 0$) obviously coincide with those of the principal determinant D of this linear system. It is straightforward to find that

$$D \propto \sin k \left\{ 2(1 - \lambda)t - \lambda^2 \sum_{i=1}^{M_d} \frac{a_L^{(i)} a_R^{(i)}}{\epsilon - E_i} \right\} \prod_{l=1}^{M_d} (\epsilon - E_l), \quad (7)$$

where $\epsilon = -t \cos k$. We will now analyse this expression in the two limiting cases.

$\lambda \ll 1$ – *weakly coupled dot*. As λ decreases, the zeroes $\epsilon = Z_i$ approach the dot levels, $\epsilon = E_i$. To leading order in λ , we find $Z_i = E_i + \lambda^2 a_L^{(i)} a_R^{(i)} / (2t)$. Thus, (i) the direction in which the transmission zero is shifted with respect to the corresponding dot level E_i is determined solely by the sign of the product of the tunnelling elements, $\sigma_i = \text{sign} a_L^{(i)} a_R^{(i)}$. We thus find that whenever all such signs are the same, each inter-level energy interval has exactly one transmission zero, whereas otherwise there arise intervals which contain either two such zeroes or none at all. (ii) Not counting the spurious zero at $k = 0$, there are exactly M_d transmission zeroes. At $\lambda \rightarrow 0$, each zero approaches the corresponding level E_i , cancelling its transmission peak and thereby restoring the featureless $t_{tr}(\mu)$ [and $\Theta_{tr}(\mu)$] at $\lambda = 0$.

$\lambda \rightarrow 1$ – *fully coupled dot*. As the value of λ increases, the transmission zeroes move further away from their corresponding dot levels. While at a finite λ they obviously

cannot cross any of the dot levels to drift into neighbouring inter-level intervals, in those intervals which contain pairs of zeroes the zeroes may meet and disappear from the real energy axis; likewise, new pairs of zeroes may appear in some inter-level intervals. In addition, one or more zeroes which at smaller λ may have been located below the lowest dot level or above the highest one may now move out of the conduction band. In the fully coupled case of $\lambda = 1$, the r. h. s. of equation (7) is proportional to the polynomial of the power $M_d - 1$, which guarantees that the maximal possible number of transmission zeroes is $M_d - 1$; this number increases to M_d for $0 < \lambda < 1$ [it follows that at $\lambda \rightarrow 1$ a transmission zero located outside the dot energy range must move out of the conduction band along the real energy axis]. When the two adjacent levels are characterised by the same signs $\sigma_i = \sigma_{i+1}$, it is certain that there is a transmission zero (or possibly an odd number of zeroes) between them; otherwise there may be either two zeroes (or, in principle, an even number of zeroes) or none.

It appears that the possibility to have more than two zeroes in any inter-level interval requires a fine-tuning of the parameters of QD, and cannot be considered as generic. Barring these special cases, we see that had we compared this unrealistic non-interacting scenario to the experimentally observed correlated occurrence of exactly one transmission zero between every two adjacent dot levels, this would indeed require all the level coupling signs, σ_i , to be the same.

Furthermore, when at $\lambda = 1$ for one of the dot levels E_i the quantity $|a_L^{(i)} a_R^{(i)}|$ is much smaller than the energy distances to the neighbouring levels, such a weakly coupled level is approached by a single transmission zero at

$$Z_i = E_i - a_L^{(i)} a_R^{(i)} \left[\sum_{l \neq i} \frac{a_L^{(l)} a_R^{(l)}}{E_i - E_l} \right]^{-1}. \quad (8)$$

We note that in this case, the direction from which the transmission zero would approach is not determined solely by σ_i .

Finally, for reference purposes we quote the full expression for the transmission coefficient of a generic dot as given by equation (5),

$$\begin{aligned} t_{tr}^{(\lambda)}(\mu) = & -i\sqrt{t^2 - \mu^2} \left[2(1 - \lambda)t + \lambda^2 \sum_{i=1}^{M_d} \frac{a_L^{(i)} a_R^{(i)}}{E_i - \mu} \right] \left\{ i(2\lambda - \lambda^2 - 2)t\sqrt{t^2 - \mu^2} \right. \\ & - \lambda^2 \sum_{i=1}^{M_d} \frac{(a_L^{(i)})^2 t + (a_R^{(i)})^2 t - 2(1 - \lambda)(\mu - i\sqrt{t^2 - \mu^2})a_L^{(i)} a_R^{(i)}}{2(E_i - \mu)} + \\ & \left. + \mu(\lambda^2 - 2\lambda)t - \lambda^4 \frac{\mu - i\sqrt{t^2 - \mu^2}}{4t} \sum_{i < l} \frac{(a_R^{(i)} a_R^{(l)} - a_R^{(l)} a_L^{(i)})^2}{(E_i - \mu)(E_l - \mu)} \right\}^{-1}. \quad (9) \end{aligned}$$

Equation (9) contains the full information about the locations of phase lapses and transmission peaks. The latter are shifted with respect to the dot energy levels E_i , but the values of these shifts contain a pre-factor of the order of $|a_L^{(j)} a_R^{(l)}|/t^2 \ll 1$ and in most cases of interest can be treated as small.

In particular, we find that at $\lambda = 1$, and $|a_{L,R}^{(i)}| \ll |E_i - E_l|$ for all i and l , the transmission phase $\Theta_{tr}(\mu)$ in the vicinity of a dot level E_i is given by

$$\tan \Theta_{tr}(\mu) = \frac{\mu}{\sqrt{t^2 - \mu^2}} + \frac{(a_L^{(i)})^2 + (a_R^{(i)})^2}{2\sqrt{t^2 - \mu^2} \left[E_i - \mu - \sum_{l \neq i} \frac{(a_R^{(i)} a_L^{(l)} - a_R^{(l)} a_L^{(i)})^2}{4(E_l - E_i)t^2} \right]}. \quad (10)$$

This corresponds to the expected smooth increase of the transmission phase by π with the value of μ increasing and sweeping E_i . When the chemical potential lies away from the band edges, $|\mu| < 1$, the width of the step is of the order of the level broadening \ddagger ,

$$\Gamma_i = \frac{(a_L^{(i)})^2 + (a_R^{(i)})^2}{2t^2} \sqrt{t^2 - \mu^2}, \quad (11)$$

and the sum in the denominator of equation (10) shifts the position of the centre of this step (coinciding with the transmission amplitude maximum) on the energy axis with respect to the bare dot level E_i .

This complex behaviour of transmission phase is exemplified by figure 2 for the case of a four-level dot with $\sigma_i = \{1, -1, -1, 1\}$. At a relatively small value of $\lambda = 0.3$ (dotted line), transmission phase remains close to zero except in the immediate vicinity of the dot levels, and there is a phase lapse of π near every level. With increasing λ , the continuous increase of Θ_{tr} by π in the vicinity of each level becomes progressively less steep, and the phase lapses shift further away from the levels. The directions and rates of these shifts reflect the differences in the coupling signs σ_i and coupling magnitudes. While for all values of λ there is exactly one phase lapse between E_2 and E_3 and none between E_3 and E_4 , the pair of phase lapses located between E_1 and E_2 approach each other, as shown by the dashed-dotted line ($\lambda = 0.75$). They eventually merge and disappear, and with further increase of λ a new pair of transmission zeroes emerges outside the dot energy range at $\mu < E_1$ (see the dashed line, $\lambda = 0.971$). With increasing λ , one of these new phase lapses moves towards E_1 , whereas the other moves rapidly to the left, disappearing in the fully coupled case of $\lambda = 1$ (solid black line). The solid green line illustrates the effect of reducing the coupling of a single dot level E_3 to the leads in the $\lambda = 1$ case. We see that the increase of transmission phase, $\Theta_{tr}(\mu)$, by π near E_3 becomes steeper as we reduce $a_{R,L}^{(3)}$, and a phase lapse approaches E_3 from the left, ‘‘annihilating’’ the smooth increase in the limit $a_{R,L}^{(3)} \rightarrow 0$. We also note that with decreasing coupling to the third QD level, the two of phase lapses located to the left of E_1 and to the right of E_4 move away from the dot levels and disappear.

In the general case of a non-interacting multi-level dot, the behaviour of $\Theta_{tr}(\mu, \lambda)$ reflects the analytical properties of the complex transmission amplitude t_{tr} , which are probably not known in detail. In any case, these properties are far too cumbersome to try and analyse the effect of charging interaction on Θ_{tr} in such a generic case. One is therefore left with the option to consider the effects of interaction in a simple model case

\ddagger This is given by $4\Gamma_i = \pi[(a_L^{(i)})^2 + (a_R^{(i)})^2]\rho(1/2)$, where $\rho(1/2)$ is the local density of states at the terminal point of a lead, *e.g.*, $d\langle \hat{c}_{1/2}^\dagger \hat{c}_{1/2} \rangle / d\mu$ at $\lambda = 1$.

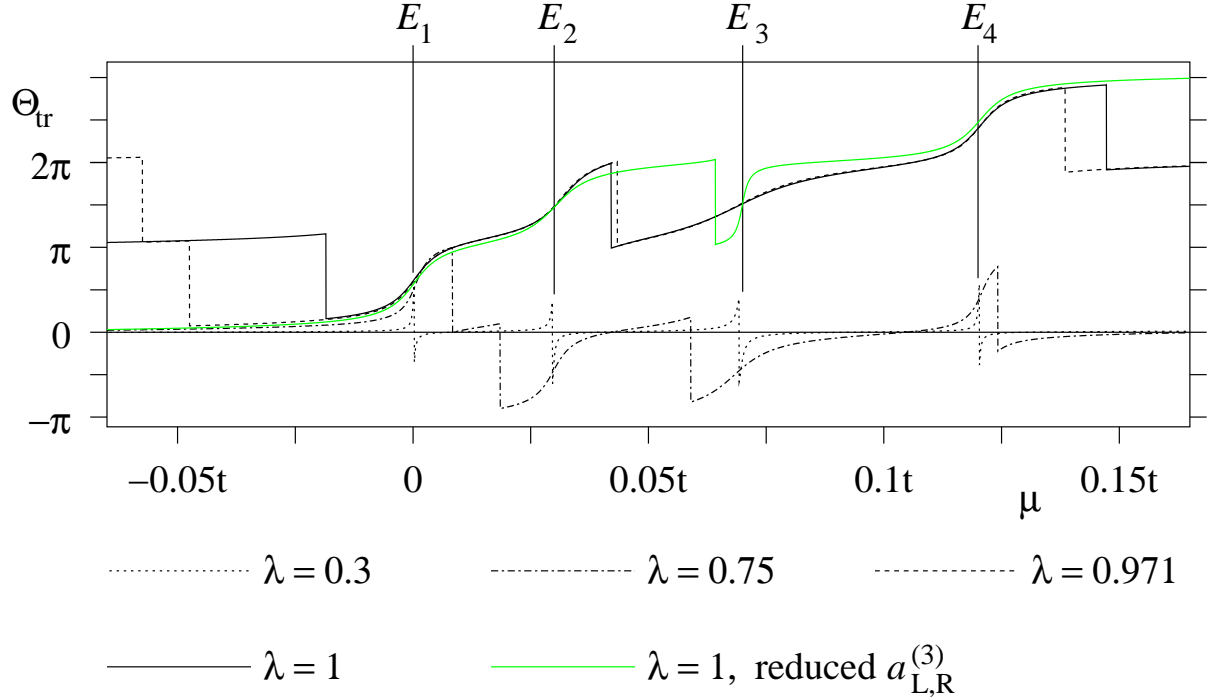


Figure 2. (colour) The complex behaviour of the transmission phase for different regimes of QD-lead coupling. The dependence of Θ_{tr} on μ for a non-interacting four-level dot with $a_L^{(i)}/t = \{0.05, 0.07, 0.1, 0.08\}$ and $a_R^{(i)}/t = \{0.08, -0.08, -0.12, 0.06\}$. The dot spectrum is given by $E_i/t = \{0, 0.03, 0.07, .12\}$. The “perturbation strength” λ (cf. figure 1) is equal to 0.3, 0.75, 0.971, and 1 for dotted, dashed-dotted, dashed, and solid black lines respectively. The green solid line corresponds to the fully coupled dot ($\lambda = 1$) with reduced values of the tunnelling matrix elements for the 3rd level: $a_L^{(3)} = 0.03t$ and $a_R^{(3)} = -0.036t$.

in order to identify the relevant correlation-induced *mechanisms* with the hope that the results will prove generic at a qualitative level.

3. The Mean Field Scheme for an Interacting Two-Level Dot

The model for a two-level interacting QD. Rotation of the fermionic operators on the dot and the “intra-dot hopping” as a measure of right-left asymmetry. Mean field decoupling and mean field equations. Invariance of the mean field scheme with respect to the choice of the basis. Properties of the effective non-interacting system.

In this section, we describe our method of calculation of the transmission phase, $\Theta_{tr}(\mu)$, for an interacting two-level QD. After introducing the model, we focus on the mean field decoupling and on the properties of the resultant non-interacting system.

The minimal model for studying the phase lapse mechanism includes a two-level QD,

$$\mathcal{H}_{QD} = (E_1^{(0)} - \mu)\hat{d}_1^\dagger\hat{d}_1 + (E_2^{(0)} - \mu)\hat{d}_2^\dagger\hat{d}_2 + U\hat{d}_1^\dagger\hat{d}_2^\dagger\hat{d}_2\hat{d}_1. \quad (12)$$

Here, the operators \hat{d}_i with $i = 1, 2$ annihilate electrons on the two dot sites (with bare energies $\{E_i^{(0)}\}$, $E_2^{(0)} > E_1^{(0)}$). The QD is coupled to the two leads by the tunnelling term

$$V_T = -\frac{1}{2}\hat{d}_1^\dagger (a_L\hat{c}_{-1/2} + a_R\hat{c}_{1/2}) - \frac{1}{2}\hat{d}_2^\dagger (b_L\hat{c}_{-1/2} + b_R\hat{c}_{1/2}) + \text{h.c.} \quad (13)$$

The operators \hat{c}_j (with half-integer j) are defined on the tight-binding sites of the left and right lead (cf. figure 1). In the $U = 0$ case, the location of the transmission phase lapse with respect to the dot levels is determined by the coupling sign, $\sigma^{(0)} = \text{sign } a_R a_L b_R b_L$; in particular, in the opposite-sign case of $\sigma^{(0)} = -1$ the phase lapse occurs outside the inter-level energy interval.

In spite of the simplicity of this model, (12–13), no exact analytical solution for general values of parameters has been found so far. In a recent paper [30], the present writers suggested a mean field approach to this problem. Here, we will further explore the generality of our mean field scheme and the physical properties of the mean field solutions.

At the outset, we confine ourselves to studying the case when the values of tunnelling couplings in equation (13) obey the following condition:

$$b_R^2 - b_L^2 = a_L^2 - a_R^2, \quad (14)$$

which corresponds to a certain 3D subspace of the full space of all values of $a_{L,R}$ and $b_{L,R}$ (the latter are assumed to be real). While we did not attempt an investigation of the case when the constraint (14) is not satisfied, there is an expectation that no significant physics is missed by making this assumption (possibly barring a few isolated singular cases), which however offers an important technical benefit. Indeed, by making an orthogonal transformation of the QD fermion operators,

$$\begin{pmatrix} \hat{d}_1 \\ \hat{d}_2 \end{pmatrix} = O \begin{pmatrix} \tilde{d}_1 \\ \tilde{d}_2 \end{pmatrix}, \quad O = \begin{pmatrix} \cos \varphi & -\sin \varphi \\ \sin \varphi & \cos \varphi \end{pmatrix} \quad (15)$$

with $\tan \varphi = (a_R - a_L)/(b_L - b_R)$ we find that the tunnelling term,

$$V_T = -\frac{1}{2} \left\{ (a_L\hat{c}_{-1/2}^\dagger + a_R\hat{c}_{1/2}^\dagger)(\cos \varphi \tilde{d}_1 - \sin \varphi \tilde{d}_2) + (b_L\hat{c}_{-1/2}^\dagger + b_R\hat{c}_{1/2}^\dagger)(\sin \varphi \tilde{d}_1 + \cos \varphi \tilde{d}_2) \right\} + \text{H.c.},$$

then reduces to a simple form,

$$V_T = -\frac{1}{2}a (\hat{c}_{-1/2}^\dagger + \hat{c}_{1/2}^\dagger) \tilde{d}_1 - \frac{1}{2}b (\hat{c}_{-1/2}^\dagger - \hat{c}_{1/2}^\dagger) \tilde{d}_2 + \text{H.c.} \quad (16)$$

At the same time, the transformation (15) changes the form of the dot Hamiltonian, equation (12), to

$$\mathcal{H}_{QD} = (\tilde{E}_1^{(0)} - \mu)\tilde{d}_1^\dagger\tilde{d}_1 + (\tilde{E}_2^{(0)} - \mu)\tilde{d}_2^\dagger\tilde{d}_2 - \frac{w_0}{2}(\tilde{d}_1^\dagger\tilde{d}_2 + \tilde{d}_2^\dagger\tilde{d}_1) + U\tilde{d}_1^\dagger\tilde{d}_2^\dagger\tilde{d}_2\tilde{d}_1. \quad (17)$$

Thus, the system can be formally viewed as a quantum dot with the “site energies” $\tilde{E}_{1,2}^{(0)}$ and the “intra-dot hopping” w_0 ; coupling to the leads is now left-right symmetric, with the “coupling sign” $\tilde{\sigma} = -1$ (figure 3). Further analysis will be carried out in terms of

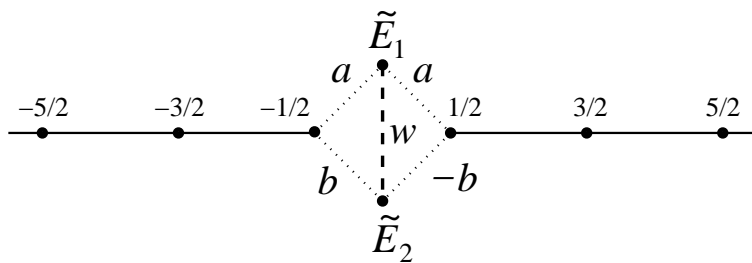


Figure 3. The model system, composed of a wire (chain) and a two-level dot, equations (16) and (17).

this new QD, assuming $\tilde{E}_2^{(0)} > \tilde{E}_1^{(0)}$. We note that the quantity

$$w_0 = \frac{1}{4} \frac{(E_2^{(0)} - E_1^{(0)})(b_L - b_R)(a_L - a_R)}{a_L(a_L - a_R) + b_L(b_L - b_R)} \quad (18)$$

is in reality a measure of left-right asymmetry of the original dot coupling, equation (13); by varying w_0 , one can probe both opposite sign ($\sigma^{(0)} = -1$) and same-sign ($\sigma^{(0)} = 1$) cases (see section 4 below).

The mean-field calculation entails decoupling the interaction term in equation (17),

$$\begin{aligned} \tilde{d}_1^\dagger \tilde{d}_2^\dagger \tilde{d}_2 \tilde{d}_1 \rightarrow & \tilde{d}_1^\dagger \tilde{d}_1 \langle \tilde{d}_2^\dagger \tilde{d}_2 \rangle + \tilde{d}_2^\dagger \tilde{d}_2 \langle \tilde{d}_1^\dagger \tilde{d}_1 \rangle - \langle \tilde{d}_1^\dagger \tilde{d}_1 \rangle \langle \tilde{d}_2^\dagger \tilde{d}_2 \rangle - \\ & - \tilde{d}_1^\dagger \tilde{d}_2 \langle \tilde{d}_2^\dagger \tilde{d}_1 \rangle - \tilde{d}_2^\dagger \tilde{d}_1 \langle \tilde{d}_1^\dagger \tilde{d}_2 \rangle + |\langle \tilde{d}_1^\dagger \tilde{d}_2 \rangle|^2, \end{aligned} \quad (19)$$

which, when substituted in equation (17), yields an effective non-interacting dot,

$$\mathcal{H}_d^{MF} = (\tilde{E}_1 - \mu) \tilde{d}_1^\dagger \tilde{d}_1 + (\tilde{E}_2 - \mu) \tilde{d}_2^\dagger \tilde{d}_2 - \frac{w}{2} (\tilde{d}_1^\dagger \tilde{d}_2 + \tilde{d}_2^\dagger \tilde{d}_1). \quad (20)$$

The self-consistency conditions take the form of three coupled mean-field equations,

$$\tilde{E}_1 = \tilde{E}_1^{(0)} + U \langle \tilde{d}_2^\dagger \tilde{d}_2 \rangle, \quad \tilde{E}_2 = \tilde{E}_2^{(0)} + U \langle \tilde{d}_1^\dagger \tilde{d}_1 \rangle, \quad (21)$$

$$w = w_0 + 2U \langle \tilde{d}_1^\dagger \tilde{d}_2 \rangle. \quad (22)$$

Here, the relevant average values are obtained from the thermodynamic potential, Ω_{MF} , of the effective non-interacting system with the Hamiltonian,

$$\mathcal{H}_{tot}^{MF} = \mathcal{H}_d^{MF} + \mathcal{H}_w + V_T + \frac{t}{2} (\hat{c}_{1/2}^\dagger \hat{c}_{-1/2} + \hat{c}_{-1/2}^\dagger \hat{c}_{1/2}) \quad (23)$$

[cf. equations (2–3)] according to

$$\langle \tilde{d}_1^\dagger \tilde{d}_1 \rangle = \partial \Omega_{MF} / \partial \tilde{E}_1, \quad \langle \tilde{d}_2^\dagger \tilde{d}_2 \rangle = \partial \Omega_{MF} / \partial \tilde{E}_2, \quad \langle \tilde{d}_1^\dagger \tilde{d}_2 \rangle = -\partial \Omega_{MF} / \partial w. \quad (24)$$

An exact and convenient method to evaluate Ω_{MF} is described in reference [30].

Clearly, the advantage of the choice (14) lies in the fact that at the mean-field level, interaction effects amount to a rather simple renormalisation of the coefficients in the single-particle part of the Hamiltonian, equation (17). We note that a similar mean field scheme can be constructed for a symmetric same-sign QD, when the constraint (14) is replaced by $a_L = a_R$, $b_L = b_R$. This case, which is analysed in reference [30], will not be discussed here; we note also that a unitary transformation of the dot operators allows one to recast the corresponding Hamiltonian in the form (16–17) with $b = 0$.

It is important to notice that had we carried out the decoupling, equation (19), in any other basis of the dot operators (including the original one, that of $\hat{d}_{1,2}$), the resultant system of mean field equations would have been equivalent to (21–22). This means that the two operations: rotating the basis [cf. equation (15)] and performing the Hartree – Fock decoupling [equation (19)] are commutative. Indeed, consider an arbitrary orthogonal transformation of the dot operators,

$$\begin{pmatrix} \tilde{d}_1 \\ \tilde{d}_2 \end{pmatrix} = O' \begin{pmatrix} d'_1 \\ d'_2 \end{pmatrix}, \quad O' = \begin{pmatrix} \cos \phi & -\sin \phi \\ \sin \phi & \cos \phi \end{pmatrix}, \quad (25)$$

in the QD Hamiltonian, equation (17). Then in the new basis of operators $d'_{1,2}$ we have:

$$\tilde{E}_1^{(0)'} = \tilde{E}_1^{(0)} \cos^2 \phi + \tilde{E}_2^{(0)} \sin^2 \phi - \frac{1}{2} w_0 \sin 2\phi, \quad (26)$$

and similar equations for $\tilde{E}_1^{(0)'}$ and w'_0 ; the interaction term remains unchanged. Now suppose that the “renormalised” quantities $\tilde{E}_{1,2}$ and w satisfy the mean field equations, (21),(22), and (24), and do the same transformation O' *after* the decoupling (19), *i.e.*, in the mean field Hamiltonian (20), yielding

$$\tilde{E}'_1 = \tilde{E}_1 \cos^2 \phi + \tilde{E}_2 \sin^2 \phi - \frac{1}{2} w \sin 2\phi, \quad (27)$$

$$\tilde{E}'_2 = \tilde{E}_1 \sin^2 \phi + \tilde{E}_2 \cos^2 \phi + \frac{1}{2} w \sin 2\phi, \quad (28)$$

$$w' = (\tilde{E}_1 - \tilde{E}_2) \sin 2\phi + w \cos 2\phi. \quad (29)$$

On the other hand, had we chosen to perform the decoupling in the $d'_{1,2}$ basis, we would have obtained the mean field equations

$$\tilde{E}'_1 = \tilde{E}_1^{(0)'} + U \partial \Omega_{MF} / \partial \tilde{E}'_2, \quad \tilde{E}'_2 = \tilde{E}_2^{(0)'} + U \partial \Omega_{MF} / \partial \tilde{E}'_1, \quad (30)$$

$$w' = w'_0 - 2U \partial \Omega_{MF} / \partial w'. \quad (31)$$

It remains to verify that the quantities $E'_{1,2}$ and w' as obtained from equations (27–29) solve the system (30–31). Since

$$\frac{\partial \Omega_{MF}}{\partial \tilde{E}'_1} = \frac{\partial \Omega_{MF}}{\partial \tilde{E}_1} \cos^2 \phi + \frac{\partial \Omega_{MF}}{\partial \tilde{E}_2} \sin^2 \phi - \frac{\partial \Omega_{MF}}{\partial w} \sin 2\phi \quad (32)$$

etc., this is easily done by a direct inspection. We conclude that the two systems of mean field equations, (21–22) and (30–31) are equivalent to each other, hence the results are indeed independent on the choice of basis. This statement illustrates the fact that our mean-field approximation is a conserving one [32], and holds also if one replaces O' in equation (25) with an arbitrary unitary matrix.

As we will see below, under certain conditions one finds that for a given value of μ , the mean field equations (21–22) for \tilde{E}_1 , \tilde{E}_2 , and w may have multiple solutions. In this case, one must choose the solution which corresponds to the lowest value of the full thermodynamic potential including the constant (non-operator) terms in equation (19),

$$\Omega = \Omega_{MF} - U \langle \tilde{d}_1^\dagger \tilde{d}_1 \rangle \langle \tilde{d}_2^\dagger \tilde{d}_2 \rangle + U \langle \tilde{d}_1^\dagger \tilde{d}_2 \rangle^2. \quad (33)$$

While the invariance of Ω_{MF} under the transformation (25) is obvious, it is straightforward to check that the sum of the last two terms on the r. h. s. also does not change, so that the entire quantity Ω is independent on the choice of basis.

Once the values of mean field parameters $E_{1,2}$ and w are determined, the transmission phase Θ_{tr} [corresponding to the effective non-interacting model (20)] can be evaluated from

$$\sqrt{t^2 - \mu^2} \tan \Theta_{tr}(\mu) = \mu + \frac{b^2(\tilde{E}_1 - \mu) + a^2(\tilde{E}_2 - \mu) + 2\mu a^2 b^2 / t^2}{(\tilde{E}_1 - \mu)(\tilde{E}_2 - \mu) - \frac{1}{4}w^2 - a^2 b^2 / t^2}. \quad (34)$$

As a function of μ , Θ_{tr} shows two smooth steps of $+\pi$ centred at the transmission peaks, $\mu = \mu_{1,2}$ with

$$\mu_{1,2} = (\tilde{E}_1 + \tilde{E}_2)/2 \mp \frac{1}{2}[(\tilde{E}_1 - \tilde{E}_2)^2 + w^2 + 4a^2 b^2 / t^2]^{1/2}. \quad (35)$$

More precisely, at $\mu = \mu_{1,2}$ the quantity Θ_{tr}/π has half-integer values. Friedel sum rule then implies [30] that the same holds for the electron population change due to the dot, $N_{dot} = N(\mu) - N_w(\mu)$, where $N(\mu)$ is the total number of carriers in the system, and $N_w(\mu)$ is the number of carriers at an unperturbed (connected) wire alone [see equation (2)], evaluated at the same value of μ .

The positions of these peaks $\mu_{1,2}$ are slightly shifted outwards with respect to the mean-field dot energy levels [eigenvalues of (20)]:

$$E_{1,2} = (\tilde{E}_1 + \tilde{E}_2)/2 \mp \frac{1}{2}[(\tilde{E}_1 - \tilde{E}_2)^2 + w^2]^{1/2}. \quad (36)$$

Equation (34) determines Θ_{tr} up to a shift by a multiple of π . One can easily investigate the evolution of $\Theta_{tr}(\mu)$ for the effective non-interacting model (20) as the “interaction strength” λ [cf. equation (5)] varies from 0 to 1. We thus find that this shift should be chosen in such a way that

$$\Theta_{tr}(\mu \rightarrow -t) \rightarrow \begin{cases} -\pi/2 & \text{for } a^2 > b^2, \\ -3\pi/2 & \text{for } a^2 < b^2. \end{cases} \quad (37)$$

In addition, at $\mu = Z$ with

$$Z = \frac{\tilde{E}_2 a^2 - \tilde{E}_1 b^2}{a^2 - b^2}. \quad (38)$$

the transmission phase suffers a lapse of $-\pi$ [*i.e.*, Θ_{tr} includes a term, $-\pi \theta(\mu - Z)$].

In the range of parameters where multiple solutions to the mean field equations arise, it is possible that, *e.g.*, $\mu = Z$ or $\mu = \mu_{1,2}$ corresponds to a thermodynamically unstable solution. This situation and its implications for the overall $\Theta_{tr}(\mu)$ profile will be discussed in greater detail in sections 5 and 6. We shall now proceed with analysing the properties of mean field solutions for various values of parameters.

4. First Mechanism for Abrupt Phase Change between Transmission Peaks: Effects of Left-Right Asymmetry And Excitonic Correlations

Overview of mean field results: “phase diagram”. Excitonic mechanism in “phase” 1: eigenstates of the dot are linear combinations of site states, hence effective coupling sign

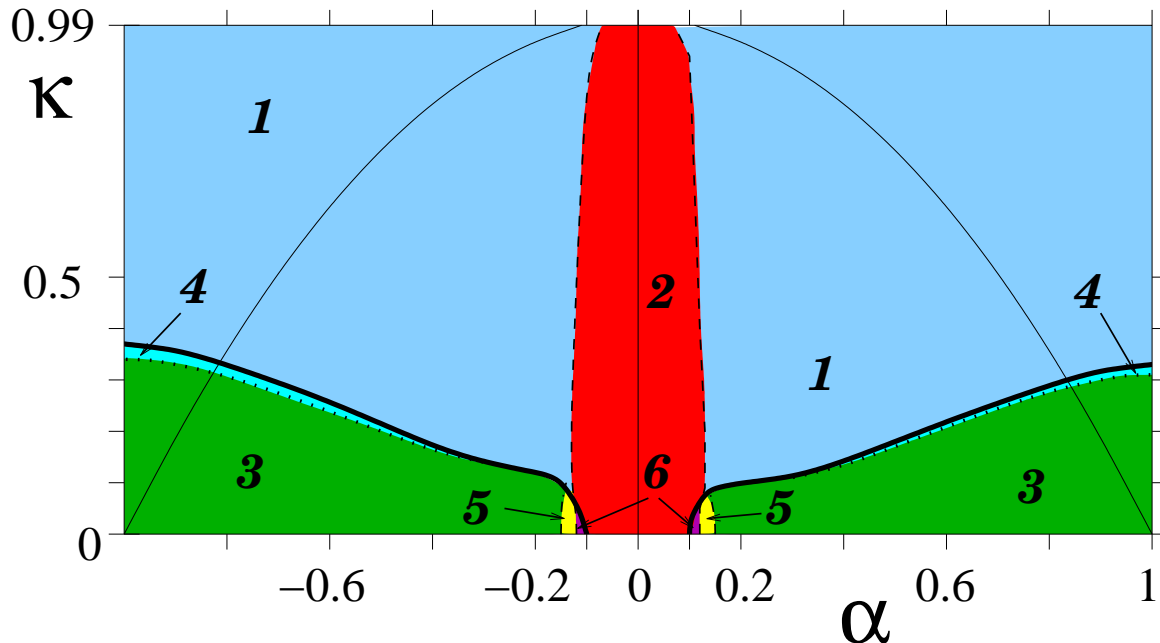


Figure 4. (colour) The “phase diagram” of a two-level QD shown in figure 3. The parameters are $U = 0.1t$, $\tilde{E}_1^{(0)} = 0$, $\tilde{E}_2^{(0)} = 0.004t$, and $\sqrt{a^2 + b^2} = 0.125t$. The axes represent the 1-2 level asymmetry, $\alpha = (|a| - |b|)/\sqrt{a^2 + b^2}$, and the dimensionless intra-dot hopping, $\kappa = w_0/[(\tilde{E}_1^{(0)} - \tilde{E}_2^{(0)})^2 + w_0^2]^{1/2}$.

change due to off-diagonal correlations on the dot. Evolution of the effective dot parameters with varying chemical potential μ . Excitonic mechanism becomes ineffective when approaching either the 1-2 or left-right symmetric situations.

We begin our discussion of the mean-field results for a two-level QD with presenting a typical mean-field “phase diagram” (figure 4). This shows how the location of the transmission phase lapse Z with respect to the two transmission peaks $\mu_{1,2}$ [see equations (35) and (38)] depends on the two dimensionless QD parameters,

$$\alpha = \frac{|a| - |b|}{\sqrt{a^2 + b^2}}, \quad \kappa = \frac{w_0}{\sqrt{(\tilde{E}_1^{(0)} - \tilde{E}_2^{(0)})^2 + w_0^2}}. \quad (39)$$

Of these, α is a measure of the 1-2 level broadening asymmetry, whereas κ is related to left-right asymmetry of the levels coupling to the two leads. In this section, we will be interested in the generic situation when κ is sufficiently large. In figure 4, this corresponds to “phases” 1 and 2 (blue and red). We will see that this typically gives rise to a hybridisation between the dot levels, which in turn results in the phase lapse of $-\pi$ occurring between the two peaks (“phase” 1). “Phase” 2, which occupies a narrow stripe near the 1-2 symmetric case, is characterised by the occurrence of a $-\pi$ -phase lapse outside the region $\mu_1 < \mu < \mu_2$.

The physics underlying this correlated restructuring of the QD spectrum at larger κ is thus somewhat similar to that of exciton formation in a semiconductor. A closer analogy can be drawn with the “excitonic correlations” between localised and extended

states in impurity problems [29]. At smaller $\kappa \rightarrow 0$ we encounter another mechanism, that of “population switching” as discussed earlier for QDs in the Coulomb blockade regime [15, 17, 27, 28] (section 5). The entire “phase diagram”, figure 4, can be interpreted in the context of interpolation between these two regimes (section 6).

Let us first formally examine the role of left-right asymmetry in our mean-field scheme, starting with equation (19). There, the diagonal and off-diagonal terms contain two types of quantum average values,

$$\tilde{n}_{1,2} = \langle \tilde{d}_{1,2}^\dagger \tilde{d}_{1,2} \rangle, \quad \tilde{n}_{12} = \langle \tilde{d}_1^\dagger \tilde{d}_2 \rangle. \quad (40)$$

In terms of the “transformed” QD, equation (17), these correspond to the two dot site occupancies, and to the intra-dot “excitonic” [29] hybridisation respectively.

Let us first suppose that the value of w_0 is sufficiently small, so that in the absence of interaction the coupling of the two QD eigenstates (36) to the dot is opposite-sign, $\sigma^{(0)} = -1$:

$$w_0^2 < (2Z^{(0)} - \tilde{E}_1^{(0)} - \tilde{E}_2^{(0)})^2 - (\tilde{E}_1^{(0)} - \tilde{E}_2^{(0)})^2, \quad Z^{(0)} = \frac{\tilde{E}_2^{(0)}a^2 - \tilde{E}_1^{(0)}b^2}{a^2 - b^2}. \quad (41)$$

In terms of figure 4, this corresponds to the area below the thin solid line. We recall that in this situation, the non-interacting dot would have the phase lapse located outside the inter-level energy interval [although strictly speaking it may still barely fall between the two transmission peaks, which are slightly shifted with respect to the dot levels, equations (36) and (35)].

As will be discussed in more detail below, the typical situation in the large-U case is that, due to large values of \tilde{n}_{12} in equation (22), w is strongly renormalised in the relevant energy region around the phase lapse. If the value of w becomes sufficiently large, the effective dot sign σ will change from -1 to 1 , for this is obviously the case for

$$|w| \gg |\tilde{E}_2 - \tilde{E}_1| \quad (42)$$

[when the product of the couplings of the two effective dot eigenstates, $(\tilde{d}_1 \pm \tilde{d}_2)/\sqrt{2}$, to the leads is given by $(a^2 - b^2)^2/4 > 0$]. The phase lapse will then be located between the two mean-field dot levels, $E_1 < Z < E_2$.

This “excitonic” mechanism of the QD sign change is operational within the blue region of our “phase diagram” (figure 4, “phase” 1), which is defined as the parameter region where the phase lapse of $-\pi$ occurs between the two transmission peaks and the properties of the effective dot vary continuously with μ . We see that this blue region extends well below the line denoting the change of the original sign, $\sigma^{(0)}$, which means that this situation is rather generic. It is further exemplified by figure 5, showing the evolution of the dot properties with μ for a particular choice of parameters.

When the chemical potential lies well below the dot levels, the latter are unoccupied and the dot parameters are close to their bare values. In particular, the “intra-dot hopping” w [solid line in figure 5 (a)] is close to $w_0 = 0.0015t$, which is small in comparison with the difference between the two “site energies” $\tilde{E}_{1,2}$ (dashed and dashed-dotted lines), $\tilde{E}_2 - \tilde{E}_1 \approx \tilde{E}_2^{(0)} - \tilde{E}_1^{(0)} = 0.004t$. This ensures that coupling to the leads

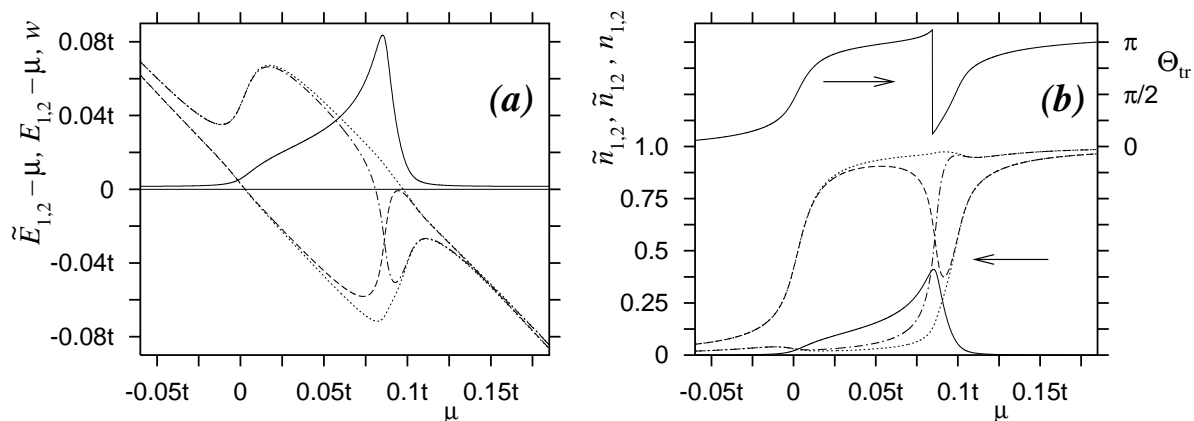


Figure 5. Mean field properties of a QD with $\alpha = 0.3$, $\kappa = 0.35$, $U = 0.1t$, $\tilde{E}_1^{(0)} = 0$, $\tilde{E}_2^{(0)} = 0.004t$, and $\sqrt{a^2 + b^2} = 0.125t$ plotted vs. chemical potential μ . (a) “Intra-dot hopping” w (solid line) and the differences between mean field “site energies” and chemical potential, $\tilde{E}_{1,2} - \mu$ (dashed and dashed-dotted lines). Dotted lines show the differences between the mean field energy levels and chemical potential, $E_{1,2} - \mu$. (b) “Off-diagonal average” \tilde{n}_{12} (lower solid line), “site occupancies” $\tilde{n}_{1,2}$ (dashed and dashed-dotted lines), and the mean-field level occupancies $n_{1,2}$ (dotted lines). The upper solid line shows the transmission phase, Θ_{tr} (right scale).

is opposite-sign, $\sigma = \sigma^{(0)} = -1$ [cf. equation (41)]. The wave function of the lower QD eigenstate in this regime is mostly localised on the site 1 of the QD, which for our choice of $\alpha = 0.3 > 0$ is the one that is stronger coupled to the leads ($a > b$, see figure 3); the lower level is therefore broader than the upper one [equation (11)].

With increasing μ , the population of this level [and hence the occupancy of site 1, dashed line in figure 5 (b)] begins to grow. The Coulomb repulsion term, $U\tilde{n}_1$ in the second equation (21) pushes the energy of the other site, \tilde{E}_2 , upwards, and its population \tilde{n}_2 [dashed-dotted line in figure 5 (b)] remains low. The energy \tilde{E}_1 (which is very close to the lower QD energy level, E_1) eventually crosses the chemical potential, resulting in a smooth increase of \tilde{n}_1 and of the transmission phase Θ_{tr} [upper solid line in figure 5 (b)] in agreement with the Friedel sum rule [30].

While the average of the two dot energy levels, $(\tilde{E}_1 + \tilde{E}_2)/2$ [see equation (36)] does not depend on w , the energy of the lower level \tilde{E}_1 goes down when w increases, making such an increase energetically favourable in the partially-occupied regime of $0 < \tilde{n}_1 + \tilde{n}_2 < 2$. We see that indeed the value of w begins to increase with increasing μ , which is accompanied by an increase of hybridisation [off-diagonal average value \tilde{n}_{12} , lower solid line in figure 5 (b)]. The nature of eigenstates begins to change continuously, and it is no longer possible to identify the lower eigenstate with site 1; at the same time, a large difference arises between the site energies $\tilde{E}_{1,2}$ and the energy eigenvalues $E_{1,2}$ [dotted lines in figure 5 (a)]. While both the site energies $\tilde{E}_{1,2}$ and site occupancies $\tilde{n}_{1,2}$ eventually cross \S , which might look reminiscent of the usual population switching

\S We find $\tilde{n}_1 = \tilde{n}_2$ at $\mu \approx 0.0859t$. The hybridisation reaches a maximum of $\tilde{n}_{12} \approx 0.411$ at $\mu \approx 0.0852t$, where $\tilde{n}_1 - \tilde{n}_2 \approx 0.1$.

scenario [15, 17, 27, 28] (see also section 5), the eigenvalues $E_{1,2}$ never coincide with each other, and the same holds for the respective level occupancies,

$$n_{1,2} = \frac{1}{2}(\tilde{n}_1 + \tilde{n}_2) \pm \frac{1}{2}\sqrt{(\tilde{n}_1 - \tilde{n}_2)^2 + 4(\tilde{n}_{12})^2} \quad (43)$$

[dotted lines in figure 5 (b)].

In particular, near the crossing point $\tilde{E}_1 = \tilde{E}_2$ the level energies $E_{1,2}$ are pushed far apart by a large w , which peaks in this region, thereby satisfying condition (42). Hence the dot becomes same-sign, $\sigma = 1$, and when (also in this region of values of μ) the $-\pi$ -phase lapse occurs with chemical potential crossing the transmission zero, the latter is located between the two level energies/transmission peaks.

With a further increase of μ , the population of the QD increases towards $\tilde{n}_1 + \tilde{n}_2 = 2$, and the energy gain associated with large w becomes less pronounced. The value of w thus begins to decrease towards w_0 , and it is in this region that the second level crossing, $E_2 = \mu$, occurs, accompanied by another smooth increase in Θ_{tr} . The site energies $\tilde{E}_{1,2}$ eventually cross again at $\mu \approx 0.145t$, reverting to their original order.

The presence of the $\sigma^{(0)} = 1$ area in figure 4 (above the thin solid line) is indicative of the fact that our Hamiltonian, equation (17), which is characterised by the opposite-sign “site coupling”, $\tilde{\sigma} = -1$, is suitable for probing both same-sign and opposite-sign original level coupling cases. We note that in figure 4, most of the $\sigma^{(0)} = 1$ area is occupied by “phase” 1.

The mechanism of interaction-induced coupling sign change becomes ineffective when approaching the line $\alpha = 0$, corresponding to equal absolute values of coupling of the two QD sites to the leads. The reasons for this are two-fold: (i) a stronger increase in $w/|\tilde{E}_2 - \tilde{E}_1|$ is required to reach the coupling sign change in this case. (ii) in parallel with the usual “population switching” scenario, when the difference in the broadening of the two levels becomes smaller, larger U is needed to make the values of \tilde{E}_1 and \tilde{E}_2 cross. Thus if $|\alpha|$ is decreased while U is kept constant, the site energies $\tilde{E}_{1,2}$ cease to cross, and in the partially-filled QD regime stay progressively further away from each other. This decreases the level overlap and hence the ability of the system to form \tilde{n}_{12} and thereby renormalise w . At the same time, the energy gain associated with larger w in the partially-filled region becomes smaller.

Thus the coupling sign change does not occur for a relatively narrow “red” region (“phase” 2) around the $\alpha = 0$ line in figure 4, where the phase lapse of $-\pi$ is located outside the energy interval between the two transmission peaks, $\mu_1 < \mu < \mu_2$. “Phase” 2 is also characterised by a continuous evolution of the dot properties with varying μ . The area occupied by “phase” 2 becomes smaller with increasing U or $|w_0|$; it is located below the line denoting the sign change $\sigma^{(0)} = -1 \rightarrow \sigma^{(0)} = 1$.

This “excitonic” mechanism also breaks down when approaching the $w_0 = 0$ line. The reason for this is clear from figure 3: at $w = 0$, the contribution of the two virtual hopping paths (via the lead sites $\pm 1/2$) cancel each other, owing to the difference in the signs of coupling of site 2 to the right and left leads. Thus if we start with the $w_0 = 0$ case, a non-zero off-diagonal average value \tilde{n}_{12} cannot be formed, and w remains equal

to zero for all values of μ [see equation (22)]. Equivalently, in the $w_0 = 0$ case the dot sites 1 and 2 are coupled to even and odd combinations of electron wave functions in the two leads respectively; phases of these combinations remain fully independent of each other.

It is, however, precisely in this region of small w_0 that the “population switching” mechanism becomes operational in its conventional form. In order to further understand the structure of our “phase diagram”, figure 4, we now have to proceed with a more detailed analysis of the $w_0 = 0$ case.

5. Second Mechanism for Abrupt Phase Change between Transmission Peaks: Population Switching in the Symmetric Case – Discontinuous vs. Continuous Scenario

“Population switching” in the right-left symmetric case. Evolution of the effective dot parameters in the discontinuous case. Multiple mean field solutions and the phase lapse renormalisation. Origins of the discontinuity. Continuous population switching in the absence of the Coulomb blockade. Effects of population switching and excitonic correlations on the transmission amplitude. Summary: excitonic correlations, continuous and discontinuous population switching.

We will now consider the behaviour of an interacting two-level dot in the right-left symmetric case of $w_0 = 0$. This situation was addressed earlier [15, 17, 27, 28], and the associated notions of “hovering level” [15] or “population switching” [17] were advanced in the literature. Nevertheless until recently [30, 33] no clear distinction has been made between the two scenarios of continuous and discontinuous population switching. We will see that the difference between these two behaviours affects the magnitude of transmission phase lapse. More generally, the behaviour of a right-left symmetric QD turns out to be qualitatively different from the one found in the larger w_0 regime (coupling sign change due to “excitonic” correlations, section 4). Once we clarify the effects of interaction at $w_0 = 0$, the entire “phase diagram”, figure 4, can be understood in terms of interpolation between these two regimes (section 6).

The mean-field analysis reported here has its obvious shortcomings. It is known ([20, 21, 22, 23, 24, 25], some of these references include approximate methods) that at least within a certain parameter range the discontinuity is smoothed (see also section 7 below). We include our mean-field results here as a convenient reference point for more elaborate analyses. We also note that available studies of the effects of quantum fluctuations [20, 21, 22, 23, 24, 25] are not sufficient to conclude that the discontinuous evolution as described below is *always* an artifact of mean-field, to be “cured” in a more proper treatment.

We already pointed out that in the $w_0 = 0$ case the off-diagonal average value vanishes identically, $\tilde{n}_{1,2} = 0$, resulting in turn in the absence of effective intra-dot hopping, $w = 0$ [equation (22)]. The “site energies” therefore coincide with the mean-

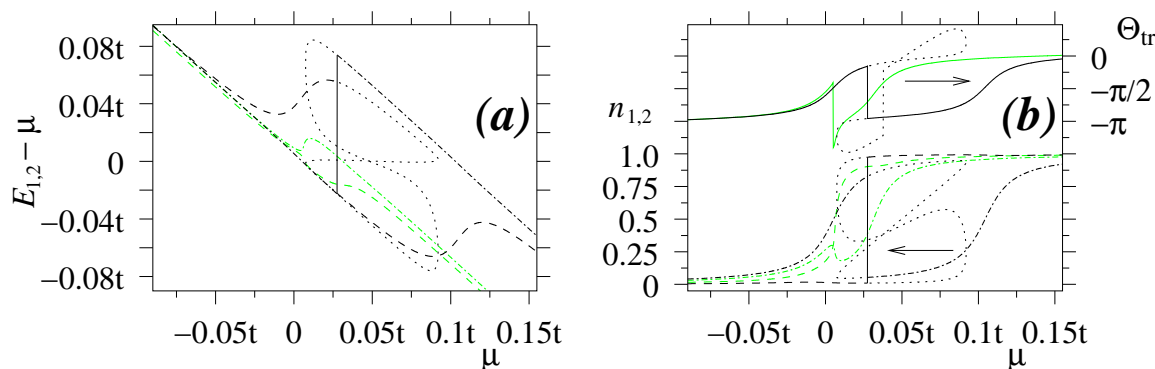


Figure 6. (colour) Mean-field properties of a two-level QD with right-left symmetry, plotted vs. chemical potential μ (black lines). QD parameter values are $\alpha = -0.6$, $w_0 = 0$, $U = 0.1t$, $\tilde{E}_1^{(0)} = 0$, $\tilde{E}_2^{(0)} = 0.004t$, and $\sqrt{a^2 + b^2} = 0.125t$. (a) the differences between mean field energy levels and chemical potential, $E_{1,2} - \mu$ (dashed and dashed-dotted lines). (b) Level occupancies, $\tilde{n}_{1,2}$ (dashed and dashed-dotted lines). The solid line shows the transmission phase, Θ_{tr} (right scale). In both (a) and (b), black dotted and vertical solid lines denote the unstable solution and the discontinuous change of the QD state respectively, whereas the respective green lines correspond to the continuous-evolution case of smaller U and smaller $|\alpha|$, *viz.* $U = 0.03t$, $\alpha = -0.25$.

field QD energy levels, $E_{1,2} = \tilde{E}_{1,2}$, and the same holds for site and level occupancies, $\tilde{n}_{1,2} = n_{1,2}$ [see equations (36) and (43)]. Since there is no hybridisation, the eigenstates of the QD do not change for all values of μ , and their respective couplings to the leads remain constant (no interaction-induced sign change can occur). Thus, the coupling of our QD to the leads remains opposite-sign, so that the transmission zero Z , equation (38), always lies outside the energy interval between the mean field QD energy levels, on the side of the weaker-coupled level (*i.e.*, for $|a| < |b|$ we find $Z < E_{1,2}$ if $E_1 < E_2$, and $Z > E_{1,2}$ in the opposite case of $E_1 > E_2$).

Typical behaviour of $E_{1,2}(\mu)$ and $n_{1,2}(\mu)$, as well as that of the transmission phase, $\Theta_{tr}(\mu)$, is shown in figure 6. The figure corresponds to the $\alpha < 0$ case, when the coupling of the upper bare dot level (dot site 2) to the leads is stronger than that of the lower one, $|b| > |a|$ [equation (39)]. We will now trace the changes of mean-field QD parameters with increasing μ , addressing first the case of stronger interaction effects (larger values of U and $|\alpha|$), as shown in figure 6 by the black lines. We also refer to figure 7 for a schematic representation of the corresponding changes in the mutual orientations of the two dot levels $E_{1,2}$, transmission zero Z and chemical potential μ .

(i) When the chemical potential is well below the bare QD energy levels, $\mu < E_{1,2}^{(0)}$, the dot contribution to the overall density of states at the Fermi level comes mainly from the tail of the broader level E_2 . Therefore the occupancy of the dot site 2 [black dashed-dotted line in figure 6 (b)] has a larger value, and with increasing μ increases at a higher rate, than that of site 1 (black dashed line). Owing to the large value of U , the mean field equations (21) then dictate that the mean field QD level energies E_1 and E_2 [dashed and dashed-dotted lines in figure 6 (a)] eventually cross, $E_1 > E_2$ for

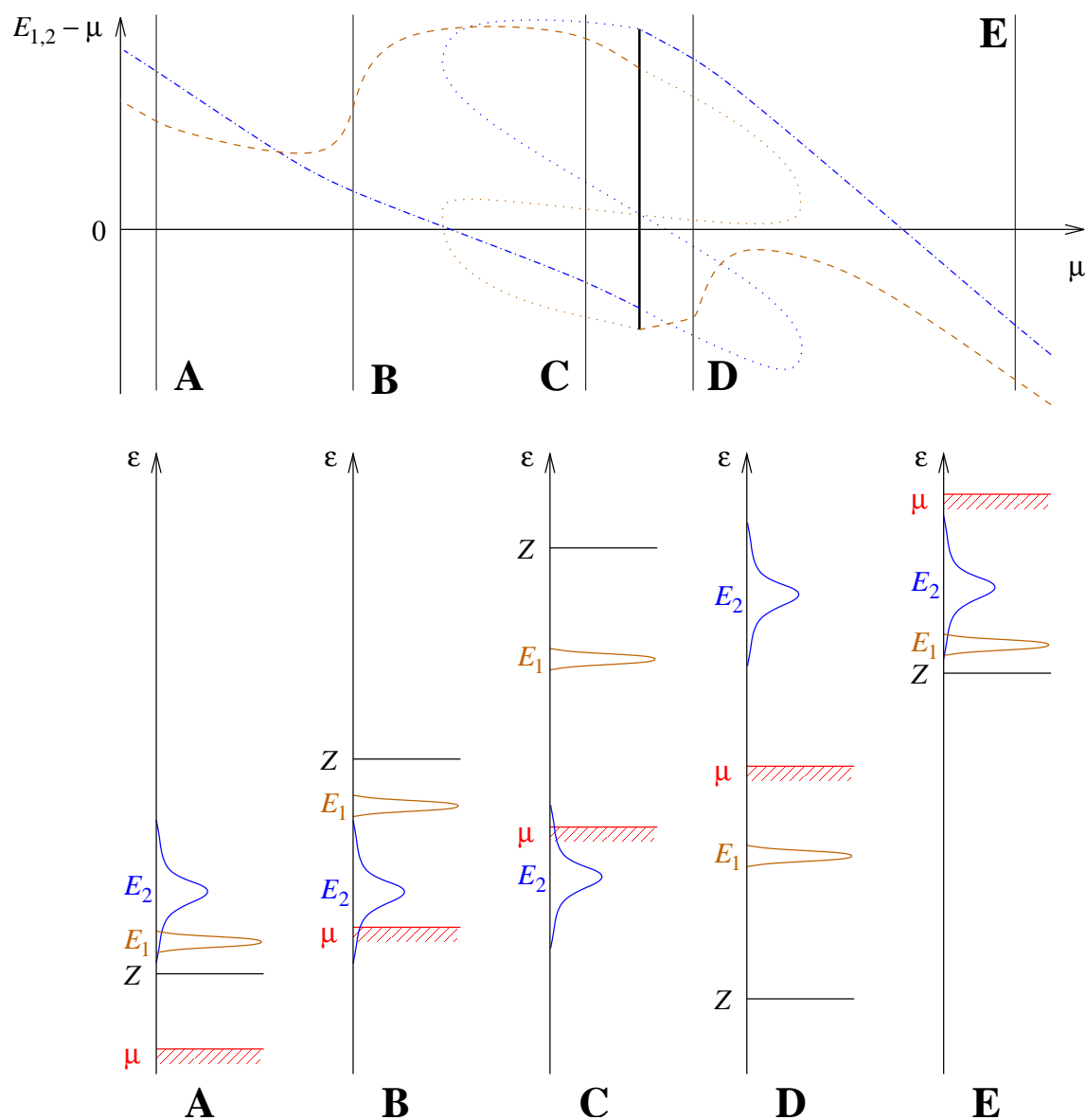


Figure 7. (colour) Discontinuous population switching: schematic representation of the chemical potential dependence of the two level energies $E_{1,2}$ (dashed and dashed-dotted lines; it is assumed that the dot-lead couplings of levels 2 and 1 satisfy $b > a$). Dotted lines correspond to the unstable solution, whereas the discontinuity is marked by a bold vertical line. In the lower part, locations of $E_{1,2}$, μ and the transmission zero Z are depicted schematically for five points A-E, showing explicitly the QD level rearrangement along with the switching in the location of Z .

$\mu > -0.8t$. The smooth increase of the dot population, and hence of the transmission phase $\Theta_{tr}(\mu)$ [black solid line in figure 6 (b)], continues beyond this crossing point. (see also figure 7, points A, B).

(ii). With further increase of μ , the lower mean-field level E_2 crosses the Fermi level at $\mu = 0.0052t$, resulting in the usual feature (shoulder) in Θ_{tr} . While $n_2(\mu)$ grows apace with Θ_{tr} , the value of $n_1(\mu)$ remains low, passing through a maximum of $n_1 \approx 0.017$ at $\mu \approx -0.01t$. The transmission zero Z remains well above the Fermi level, $Z > E_1 > \mu$ (figure 7, points B, C). At $\mu > 0.0075t$, two additional solutions to the mean field equations appear [dotted lines in figures 6 (a) and (b)]. At the beginning, these new solutions are characterised by higher values of the total energy, $\Omega(\mu)$, which can be evaluated via equation (33).

(iii). As can be anticipated by considering the filled dot case at $\mu \gg E_{1,2} \approx E_{1,2}^{(0)} + U$, with increasing μ the energy levels $E_{1,2}$ must eventually cross again, reverting to their original order (cf. figure 7, point E). In the present case, this second crossing occurs in a discontinuous manner, i.e., at some point it becomes energetically favourable to abruptly depopulate level 2 (which then shifts upwards) while putting most of the carrier population of the dot into level 1 (which is lowered). This is the “*population switching*” in its discontinuous form as proposed in reference [17]. Mathematically, with increasing μ within the multiple-solution region we eventually reach the point $\mu_c \approx 0.0275t$, where the total energy values of the two lower-energy solutions cross. Hence a switch of the solution branch occurs, accompanied by a discontinuous change in all the QD properties (vertical solid lines in figure 6). While on approach to this critical value of μ from below the Fermi level was located below the transmission zero, the situation immediately following the transition is that of $Z < E_1 < \mu < E_2$, i.e., the Fermi level is above the point of transmission phase lapse. The actual point $Z = \mu$ (and the associated phase lapse of $-\pi$), however, is never crossed because it lies in the thermodynamically unstable region. This is illustrated by the dotted line showing transmission phases for unstable solutions in figure 6 (b), which includes a phase lapse of $-\pi$ at $\mu \approx 0.038t$. The actual change of transmission phase at $\mu = \mu_c$,

$$\Delta\Theta_{tr} = -\pi + \pi\Delta N_{dot} \quad (44)$$

includes both the contribution of this phase lapse and another term, related by the Friedel sum rule [30] to the jump of the “dot-related” particle number, $N_{dot} = N(\mu) - N_w(\mu)$. Here, $N(\mu)$ is the total number of particles in the system, whereas N_w is the number of particles in an unperturbed (connected) wire, equation (2). Thus, N_{dot} includes both the dot occupancy, $n_1 + n_2$, and the “dot-induced” change of population within the leads. N_{dot} must always increase with decreasing gate voltage, or equivalently with increasing μ ; in particular, it has a positive jump at $\mu = \mu_c$, renormalising the value of phase jump $\Delta\Theta_{tr}$, equation (44). In our case, $\Delta\Theta_{tr} \approx -2.514$, hence $\Delta N_{dot} \approx 0.20$ [note the difference of the latter from the jump in the dot level occupancy, $\Delta(n_1 + n_2) \approx 0.28$]. In the schematic representation on figure 7, the discontinuity (bold vertical line) occurs between the points C and D.

(iv) With further increasing μ , the (narrower) dot level 1 remains nearly filled, although its occupancy $n_1(\mu)$ does not vary monotonously, passing through a local minimum of $n_1 \approx 0.987$ at $\mu \approx 0.12t$; the corresponding energy level E_1 lies below the Fermi level. The occupancy of the other level, n_2 , increases with μ , with the level E_2 crossing the chemical potential at $\mu \approx 0.103t$, resulting in another smooth increase of Θ_{tr} . We note that the same (broad) level E_2 crossing the Fermi level *twice* (above and below the jump) is a known feature (“hovering level”) of the population switching scenario [15, 17]. The unstable solutions (dotted lines) provide a continuous connexion between the states of the system above and below the jump, with the level E_1 crossing the Fermi level at $\mu \approx 0.089t$ (in the unstable region). With increasing μ , the pair of unstable solutions finally disappears at $\mu \approx 0.092t$. In figure 7, the second level crossing and the disappearance of the unstable solution occur between points D and E.

The origins of discontinuity as found at $\mu = \mu_c$ become clear if one considers the case when one of the QD levels is fully decoupled from the rest of the system, *e. g.*, $a = 0$ (corresponding to $\alpha = -1$) and $w_0 = 0$. With increasing μ , the occupancy of the QD level 1 then changes abruptly from $n_1 = 0$ to $n_1 = 1$, at which point all other QD properties (n_2 , $E_{1,2}$, Θ_{tr}) must suffer a jump as well. In the language of mean field (which is exact in this case as there are no quantum fluctuations of n_1), this means the presence of multiple solutions in a finite region of values of μ near the jump point [17]. Indeed, assuming that the QD energy scales $E_2^{(0)} - E_1^{(0)}$, b^2/t , and U are all much smaller than the bandwidth, $2t$, we find that the value of $E_1(\mu)$ is determined by a single mean field equation,

$$E_1 = E_1^{(0)} + U \left\{ \frac{1}{2} + \frac{1}{\pi} \arctan \left[\frac{\pi \nu_0}{b^2} \left(E_2^{(0)} + U \theta(\mu - E_1) - \mu \right) \right] \right\}, \quad (45)$$

where ν_0 is the per-site density of states in the leads. It is easy to verify that there is at least one multiple solution region, where the system switches from the $E_1 > \mu$ to $E_1 < \mu$ branch. These two branches of $E_1(\mu)$, connected by a segment of the singular line $E_1(\mu) = \mu$ (where in the $a = 0$ case the value of n_1 is ill-defined) together form a z-shaped structure similar to that shown in figure 6 (or, in a cartoon form, in figures 7 and 9 below). When the value of α is increased from $\alpha = -1$ (corresponding to $a \neq 0$), this picture changes in a continuous fashion, so that in order to eliminate the multiple solution region (and hence the jump) altogether, a must exceed a certain finite value, $a > a_0(U)$. In the opposite case of $a < a_0$, the discontinuity persists, as exemplified by the $\alpha = -0.6$, $U = 0.1t$ case shown in figure 6 (black lines) and discussed above.

If in the latter case of $\alpha = -0.6$, $U = 0.1t$ the value of α is increased further, one finds that the while the absolute value of the jump decreases (and the phase lapse value approaches $-\pi$), the location of the discontinuity shifts further to the left. By the time the discontinuity disappears at $\alpha_c(U) \approx .012$, the phase lapse is outside the interval of the values of μ between the two transmission peaks. This situation changes when the value of U is smaller; we will now turn to the $\alpha = -0.25$, $U = 0.03t$ case, shown in figure 6 by the green lines.

In this case, the mean field energy levels E_1 and E_2 [green dashed and dashed-dotted

lines in figure 6 (a)] do not cross, $E_1 < E_2$ for all values of μ . Nevertheless, they do come close to each other at $\mu \approx -0.0025t$, where $E_2 - E_1 \approx 0.0014t$; a slight increase in $|\alpha|$ would give rise to a pair of crossings, $E_1 = E_2 > \mu$, in this region, without changing the overall picture. Throughout this low- μ region (where the electron population on the dot, $n_1 + n_2$, is below 0.5), the occupancy n_2 of the broader level 2 [green dashed-dotted line in figure 6 (b)] is larger than that of site 1 (green dashed line). The value of E_1 crosses μ at $\mu \approx 0.007t$; this is accompanied by a rapid increase in the value of n_1 , which exceeds n_2 for $\mu > 0.05t$, giving rise to a sharp upturn in $E_2(\mu)$ [cf. equation (21)]. Around this point, it becomes favourable to depopulate level 2 (hence a downturn in n_2) while increasing n_1 . This process however happens continuously, exemplifying the scenario of *continuous population switching*, as encountered earlier in references [27, 28]. Comparing this scenario with that of $U = 0.1t$, $\alpha = -0.6$ discussed above, one may say that a slight non-monotonicity of $n_{1,2}(\mu)$ noted in that case developed presently into the sharp maximum of n_2 at $\mu \approx 0.04t$ and absorbed the jump in the level occupancies.

With a further increase of μ , level 1 remains nearly filled, whereas n_2 eventually starts to grow again, with E_2 crossing the Fermi level around $\mu \approx 0.03t$. This is accompanied by an increase in E_1 , with the difference $E_2 - E_1$ approaching its bare value, $E_2^{(0)} - E_1^{(0)} = 0.004t$, as the chemical potential increases beyond the dot energy range.

Throughout the entire range of values of μ , the transmission zero is located below the lower dot level, $Z < E_1$. We note, however, that the points $\mu = \mu_{1,2}$ as defined by equation (35) (which we use as transmission peak locations, see below), are shifted with respect to those of the dot levels. This shift becomes relatively more pronounced when the dot levels lie close to each other (on the scale of the level widths), and if the value of α is not too large, the phase lapse may fall in between the two transmission ‘‘peaks’’ while remaining outside the interval between the two dot levels. This situation is realised in the present case, where the transmission phase [solid green line in figure 6 (b)] suffers a lapse of $-\pi$ at $\mu \approx 0.005t$ (the point where $n_1 = n_2$), shortly above the point of $\mu = \mu_1 \approx 0.002t$. We note a strong asymmetry of the ‘‘peak’’, reflected in a rather irregular profile of $\Theta_{tr}(\mu)$ near the phase lapse. The rapid non-monotonous variation of the dot parameters, combined with a rather small inter-level distance $E_2 - E_1$, results also in the absence of a well-defined ‘‘shoulder’’ of $\Theta_{tr}(\mu)$ associated with the second transmission peak; the value of μ_2 is about $0.034t$.

These features are further illustrated by a plot of the transmission amplitude $|t_{tr}(\mu)|$,

$$|t_{tr}|^2 = (t^2 - \mu^2) \left[\frac{b^2}{t^2}(\tilde{E}_1 - \mu) - \frac{a^2}{t^2}(\tilde{E}_2 - \mu) \right]^2 \left\{ \left[\frac{a^2}{t^2}(\tilde{E}_2 - \mu) + \frac{b^2}{t^2}(\tilde{E}_1 - \mu) + 2\mu \frac{a^2 b^2}{t^4} \right]^2 \times \right. \\ \left. \times (t^2 - \mu^2) + \left[(\tilde{E}_1 - \mu + \frac{a^2}{t^2}\mu)(\tilde{E}_2 - \mu + \frac{b^2}{t^2}\mu) - (t^2 - \mu^2) \frac{a^2 b^2}{t^4} - \frac{1}{4}w^2 \right]^2 \right\}^{-1} \quad (46)$$

as a function of μ (figure 8), where the case of $U = 0.03t$, $\alpha = -0.25$ is represented by the dashed line. We see that in this case, $|t_{tr}|$ does not show the two well-separated peaks

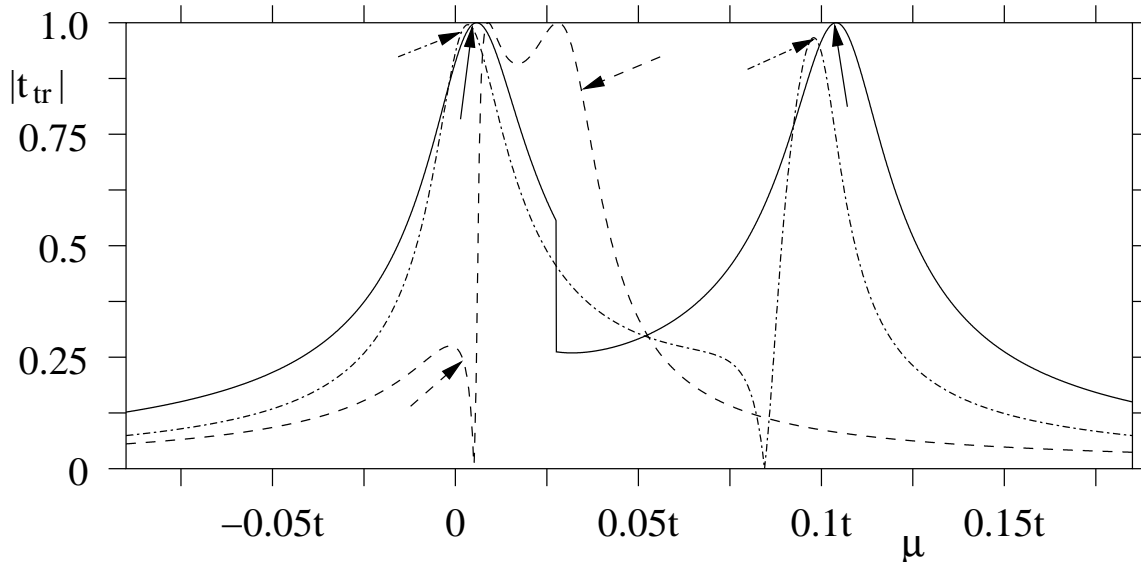


Figure 8. Transmission amplitude $|t_{tr}$ for an interacting two-level QD as a function of chemical potential: solid line, $\alpha = -0.6$, $U = 0.1t$, and $w_0 = 0$; dashed line, $\alpha = -0.25$, $U = 0.03t$, and $w_0 = 0$; dashed-dotted line, $\alpha = 0.3$, $U = 0.1t$, and $\kappa = 0.35$ (corresponding to $w_0 = 0.0015t$). The rest of parameters for all three cases are $\tilde{E}_1^{(0)} = 0$, $\tilde{E}_2^{(0)} = 0.004t$, and $\sqrt{a^2 + b^2} = 0.125t$. The arrows show the locations of the corresponding transmission peaks as given by equation (35).

as anticipated in the Coulomb blockade regime. This is due to a relatively small value of U (and hence the small mean-field level separation). We also note that the profile of transmission is rather irregular. The points marked by the dashed arrows [locations of $\mu_{1,2}$ as given by equation (35)] do not correspond to any particular features of the plot. This is not surprising, since these values of $\mu = \mu_{1,2}$ correspond to half-integer values of N_{dot} and should approach the transmission peak locations in the Coulomb blockade regime only.

We note the presence of a transmission zero, corresponding to a phase lapse; this is surrounded by the two peaks reminiscent of “correlation induced resonances” which were first reported in reference [20] and subsequently explained by the Kondo-type physics [24, 25].

The solid line in figure 8 corresponds to the discontinuous population switching case of $U = 0.1t$ and $\alpha = -0.6$. We see the two well-separated Coulomb blockade peaks of roughly the same width, whose maxima lie very close to the values of $\mu_{1,2}$, equation (38). As expected [30, 33], there is no transmission zero, since the actual $t_{tr}(\mu) = 0$ point belongs to the unstable solution. The discontinuity is clearly seen on the plot. An interesting feature of both dashed and solid curves in figure 8 is the presence of two maxima where the value of $|t_{tr}(\mu)|$ exactly equals one. An investigation of equation (46) suggests that this is always the case for the symmetric situation ($w_0 = 0$), provided that the mean field value of $|\tilde{E}_2 - \tilde{E}_1|$ (which in the partially filled regime is of the order of U) is larger than $|2ab/t|$ (here, we assume that both $|E_1 - E_2|$ and $(a^2 + b^2)/t$ are much

smaller than the bandwidth of the leads, $2t$).

This situation changes in the asymmetric, $w_0 \neq 0$ case, as exemplified by the dashed dotted line in figure 8. This line, which illustrates the effect of interaction-induced “excitonic correlations” (as discussed in section 4 above) shows two clear Coulomb blockade peaks of unequal height, with a transmission zero in between. Again, equation (35) gives accurate values for the peak locations.

* * *

We are now in a position to summarise the behaviour of an interacting two-level dot in the three regimes considered thus far:

(a). Right-left asymmetry ($w_0 \neq 0$), excitonic correlations (section 4). Within “phase” 1 of figure 4, this yields a phase lapse of $-\pi$ between the two transmission peaks. The underlying mechanism is the interaction-induced change in the sign of the dot-lead coupling, the evolution of dot parameters with varying μ is continuous throughout, the transmission peaks are of unequal height and are separated by a transmission zero.

(b). Right-left symmetric ($w = 0$) case showing a discontinuous QD level population switching as a function of μ . The locus of the corresponding points in figure 4 is at the lower edge of the green area marked as “phase” 3. While the interaction-induced sign change is impossible, the phase lapse is located between the two transmission peaks of height $|t_{tr}| = 1$, due to the re-ordering of respective locations of the peaks and the transmission zero at the point of discontinuity. The latter coincides with the phase lapse (whose magnitude is however reduced to a quantity between $-\pi$ and 0) and with the transmission minimum (where the transmission amplitude retains a finite value).

(c) Continuous population switching. This case would appear at a “phase diagram” for a lower value of U as the interval of the $\kappa = 0$ axis where the blue region of “phase 1” extends all the way down to this axis. While the example we considered lies outside the Coulomb blockade region, one observes a phase lapse of π , coinciding with a transmission zero and surrounded by the “peaks” of transmission. This mechanism is driven by a strong non-monotonicity of the QD level occupancies in this regime.

Scenarios (a) and (c) are both continuous and can be expected to be robust with respect to quantum fluctuations (not included in the present treatment). This may not be the case for the discontinuous scenario (b), which is therefore likely to be partly replaced with scenario (c).

We now turn to the intermediate values of κ in order to understand the structure of the entire “phase diagram”, figure 4, in terms of interpolation between these three regimes.

6. Interplay between the Two Mechanisms: The Mean Field “Phase Diagram”

Minimal value of 1-2 asymmetry required for the correlation-induced switching in the phase lapse location. Mean field “phase diagram” as a result of superposition of the two

correlated mechanisms: descriptions of different “phases”. “Phase diagram” in the case of a smaller U and continuous population switching.

In this section, we turn to the intermediate values of κ [equation (39)] in order to understand the structure of the entire “phase diagram”, figure 4, in terms of interpolation between the different manifestations of interaction-induced correlations considered above – effective sign change due to excitonic correlations at larger κ (section 4) vs. population switching at $\kappa = 0$ (section 5).

Both of these mechanisms result in the occurrence of a phase lapse between the two transmission peaks, and the underlying physics is partially similar in that once the chemical potential lies within a (broadened) dot level, the energetically preferable situation corresponds to the broader of the two QD levels being partially filled. This in turn implies that on approach of the value of μ to the dot level energies from the side of the weaker-coupled (bare) level (*i.e.*, $\mu < E_1^{(0)} < E_2^{(0)}$ for $\alpha < 0$), a level inversion must take place, with the broader level approaching the chemical potential first. At $\kappa = 0$ (no hybridisation) this inversion takes the form of an actual level crossing, whereas at $\kappa > 0$ only the “site energies” can cross,

$$\tilde{E}_1(\mu_c) = \tilde{E}_2(\mu_c) \quad (47)$$

(figure 7, points A and B). Generally, the occurrence of the crossing, equation (47), indicates that the correlation effects are sufficiently strong to activate at least one of the mechanisms responsible for the occurrence of the phase lapse between the transmission peaks. In the case of chemical potential lying well below the dot energy levels, the two site occupancies are given by

$$\tilde{n}_1 \approx \frac{a^2 \sqrt{t^2 - \mu^2}}{\pi t^2 (\tilde{E}_1 - \mu)}, \quad \tilde{n}_2 \approx \frac{b^2 \sqrt{t^2 - \mu^2}}{\pi t^2 (\tilde{E}_2 - \mu)} \quad (48)$$

[see reference [30], equations (16-17)]. In writing equation (48) we assumed that $t \gg \tilde{E}_{1,2} - \mu$ [which allows to use the constant value $\nu_0 = 1/(\pi \sqrt{t^2 - \mu^2})$ for the density of states in the leads] and $\tilde{E}_{1,2} - \mu \gg a^2/t, b^2/t$. In addition, the value of w [equation (22)] should not be too large, $w^2 \ll a^2(t^2 - \mu^2)/t^2$ and $w^2 \ll b^2(t^2 - \mu^2)/t^2$. Since in this range of values of chemical potential w stays close to its bare value, $w \approx w_0$, [cf. figure 5] the latter is not a restrictive condition. The site energies crossing may occur below the transmission peaks only in the $a < b$ ($\alpha < 0$) case, which we will consider here. Then, equations (21) yield the following condition for the crossing point μ_c :

$$\tilde{E}_{1,2}(\mu_c) - \mu_c = \frac{U \sqrt{t^2 - \mu_c^2}}{\pi t^2} \frac{b^2 - a^2}{\tilde{E}_2^{(0)} - \tilde{E}_1^{(0)}}. \quad (49)$$

The two transmission peaks are well defined only if the dot levels are well separated at each peak. Hence the crossing point μ_c must lie well below the lowest peak, in the

|| The dependence of ν_0 on energy is indeed a weak effect, accounting for a slight asymmetry between $\alpha > 0$ and $\alpha < 0$ cases in figure 4.

region where the net occupancy of the dot, $\tilde{n}_1 + \tilde{n}_2$, is small:

$$\tilde{E}_{1,2}(\mu_c) - \mu_c \gg \Gamma_1 + \Gamma_2 = \frac{a^2 + b^2}{t^2} \sqrt{t^2 - \mu_c^2}, \quad (50)$$

where the quantity on the r. h. s. is the combined broadening of the two levels, cf. equation (11). We note that the condition (50) is also required for equations (48) to hold. In terms of our 1-2 coupling asymmetry parameter α [see equation (39)], equation (50) takes form

$$U \gg U_c \approx \frac{\pi (\tilde{E}_2^{(0)} - \tilde{E}_1^{(0)})}{|\alpha| \sqrt{2 - \alpha^2}}, \quad (51)$$

where we wrote $|\alpha|$ instead of α in order to include also the $a > b$ case, when the point μ_c lies above the transmission peaks. The value of U_c sets the scale for the interaction strength required to produce strong correlation effects. At a fixed U , these effects can be amplified by increasing the level coupling asymmetry so that

$$1 - \alpha^2 \ll 1 - \alpha_c^2 \approx \sqrt{1 - \frac{\pi^2 (\tilde{E}_2^{(0)} - \tilde{E}_1^{(0)})^2}{U^2}}. \quad (52)$$

For the values of parameters used in figure 4 this yields $\alpha_c \approx 0.09$, which is a fairly accurate estimate for the width of the red area, occupied by “phase” 2. We already mentioned that in this “phase” the phase lapse occurs outside the energy interval between the two transmission peaks, due to insufficiently strong correlation effects.

We will now turn to figure 4 and summarise the mean-field properties of QD within the parameter region corresponding to each “phase”. Typical $\Theta_{tr}(\mu)$ profiles for each of the “phases” are shown in the main panel of figure 9.

“Phase” 1 (blue). In this “phase”, a phase lapse of $-\pi$ occurs between the two transmission peaks [marked by the two boxes on the $\Theta_{tr}(\mu)$ plot]. There is no discontinuity in the evolution of other QD parameters with varying μ , as shown in figure 9 by a schematic $\mu_1(\mu) - \mu$ vs. μ plot which does not have a multiple- solution region. As explained in section 4, the underlying mechanism is that of an effective coupling sign change due to excitonic correlations, and the corresponding region is in the upper part of the “phase diagram” (larger κ), away from the $\alpha = 0$ axis.

“Phase” 2 (red). A phase lapse of $-\pi$ occurs outside the interval between the two level crossings, $\mu_{1,2}(\mu) = \mu$. The corresponding area is a narrow stripe around the $\alpha = 0$ axis, and at small or moderate values of κ its width can be estimated with the help of Eq. (52). Owing to an insufficient 1-2 level coupling asymmetry, correlation effects are not strong enough to cause either a sign change or a discontinuity (note the absence of a multiple solution region in a schematic plot of $\mu_1(\mu) - \mu$). Away from the $\alpha = 0$ axis the “site occupancies” $\tilde{n}_{1,2}(\mu)$ may still show a non-monotonous behaviour and continuous population switching (with the phase lapse located away from the transmission peaks).

“Phase” 3 (green). In this case, a “renormalised” phase lapse, $\Delta\Theta_{tr} > -\pi$, occurs between the two transmission peaks. This “phase” occupies the area adjacent to the $\kappa = 0$ axis, excluding the vicinity of the fully symmetric case, $\kappa = \alpha = 0$. The

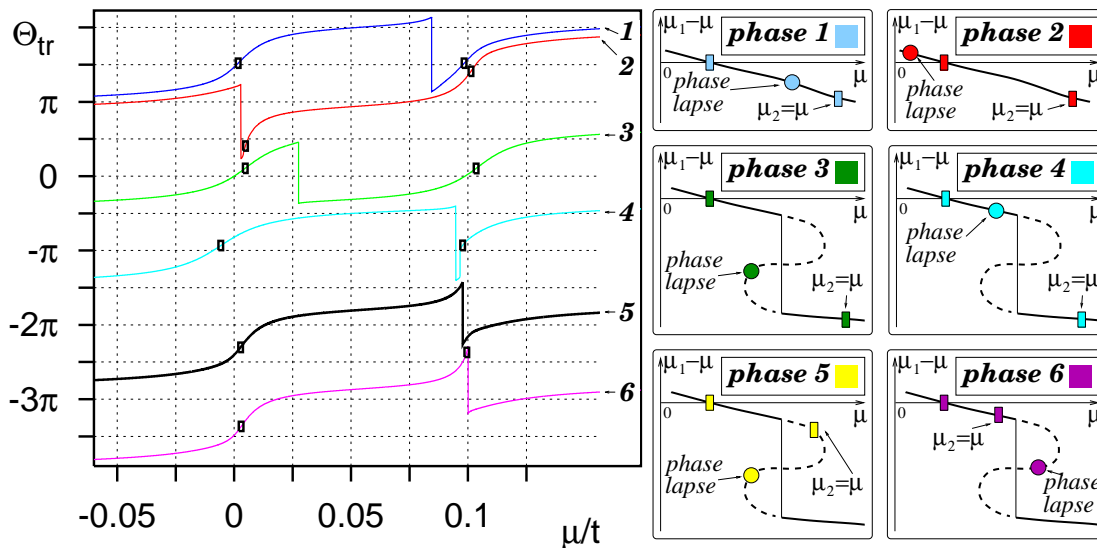


Figure 9. (colour) Typical behaviour of $\Theta_{tr}(\mu)$ in different “phases” (left; plots shifted vertically for convenience). Relative positions of transmission peaks, $\mu_{1,2}$, (boxes; also in the left panel) and the $-\pi$ -phase lapses (circles) in “phases” 1-6 are clarified by the schematic plots of $\mu_1 - \mu$ around the multiple-solution region (absent for “phases” 1-2). Solid (dashed) lines correspond to stable (unstable) solutions. The abrupt “switching” of solutions (vertical solid line) may either renormalise the phase lapse (when the $-\pi$ -lapse lies in the unstable region) or result in a positive jump of Θ_{tr} .

underlying mechanism (discontinuous population switching) was discussed in section 5. Note the presence of a “fold” on the schematic plot of $\mu_1(\mu) - \mu$, indicating the presence of a multiple solution region. The unstable part of the solution is shown by the dashed line and includes the transmission zero (circle), whereas the vertical solid line corresponds to a discontinuous jump between the two stable branches. Since at $\kappa = 0$ the multiple solution region has a finite width, the effects of right-left asymmetry (favouring the change of the coupling sign) cannot eliminate the discontinuity also at small but nonzero values of κ , corresponding to this “phase”.

The case of a fully decoupled level $\alpha = \pm 1$, $\kappa = 0$ is essentially the one considered in the reference [17] for a multi-level QD. We note that the value of phase lapse at these two points also differs from $-\pi$, contrary to earlier expectations [17]. For the values of the QD parameters used in figure 4, we find $\Delta\Theta_{tr} \approx -2.4$ at $\kappa = 0$, $\alpha = -1$, and $\Delta\Theta_{tr} \approx -2.5$ at $\kappa = 0$, $\alpha = 1$.

“Phase” 4 (cyan). This “phase” lies below the bold line which in figure 4 forms the lower boundary of the “phase” 1 area and corresponds to the onset of discontinuity in the evolution of the dot parameters with μ . With decreasing κ , this onset occurs in a continuous fashion, via the point where at some value of μ_0 the derivative of the QD parameters [such as $d\mu_1(\mu)/d\mu$] becomes infinite. With a further decrease of κ this derivative changes sign [in the case of $d\mu_1(\mu)/d\mu$, becomes positive], and a multiple

solutions area forms around μ_0 . Initially, this area is narrow and the unstable solution includes neither transmission zero nor transmission peaks (since in general μ_0 does not correspond to either of those). This is represented by the corresponding schematic plot of $\mu_1(\mu) - \mu$ in figure 9; the jump between the two branches yields a discontinuous increase of the transmission phase, $\Delta\Theta_{tr}^{(2)} > 0$, which is clearly visible in the $\Theta_{tr}(\mu)$ plot ¶ to the right of the transmission zero, $\Delta\Theta_{tr}^{(1)} = -\pi$. When the value of κ is decreased further, the unstable part of solution spreads to include the transmission zero, and we find ourselves within the “phase” 3. Since “phase” 4 interpolates between “phases” 1 and 3, it is clear that both phase jumps lie in the region between the two transmission peaks.

“Phase” 5 (yellow). This “phase” occupies the areas adjacent to those of “phase” 3 from the side of smaller values of the 1-2 level coupling asymmetry, $|\alpha|$. It lies in the discontinuous region of the “phase diagram” below the bold solid line. The decrease of $|\alpha|$ within “phase” 3 causes the discontinuity (which in this case includes a jump “over” the transmission zero) to shift towards one of the transmission peaks. Eventually the unstable area moves to include this peak as well, as can be seen from the schematic plot of $\mu_1(\mu) - \mu$. Thus the transmission peak is circumvented by a jump, as reflected by the absence of the corresponding box (and the corresponding inflexion point) on the $\Theta_{tr}(\mu)$ plot, which also includes a single renormalised phase lapse, $\Delta\Theta_{tr} > -\pi$.

“Phase” 6 (magenta). When the value of $|\alpha|$ in “phase” 5 is decreased further, the multiple solution area moves further away from the centre of the energy interval between the two transmission peaks. Eventually the unstable part (which still includes the transmission zero) clears this interval altogether, restoring the transmission peak to the stable branch. This corresponds to crossing the boundary from “phase” 5 into “phase” 6. The renormalised phase lapse, $\Delta\Theta_{tr} > -\pi$, is then located outside the area between the two peaks.

“Phase” 7 (not shown due to the small area it occupies). With a further decrease of $|\alpha|$, the multiple solution area shrinks (while shifting away from the transmission peaks), and the transmission zero returns to a stable branch. The result is similar to “phase” 4 above, with the only difference that the two phase jumps now lie outside the region between the two peaks.

A further decrease in $|\alpha|$ results in the disappearance of the multiple solution region and crossing the bold line into “phase” 2 so that the sequence of “phases” 5, 6, and 7 interpolates between “phases” 3 and 2. The seven “phases” discussed above do not exhaust all the possibilities of mutual overlaps between the multiple solution region of values of μ (and associated discontinuity), transmission zeroes, and transmission peaks. Some of the other “phases” occupy minute areas (not shown) near the crossing of the boundary between “phases” 1 and 2 and the bold line; still others do not arise for the values of parameters used in figure 4.

We see that the whole of “phase diagram”, figure 4 can be understood in terms

¶ When plotting $\Theta_{tr}(\mu)$ in this case, we used different values of the QD parameters in order to make this behaviour more pronounced.

of interpolation between the three cases: that of “phases” 2 (where the interaction does not affect the location of the phase lapse between the transmission peaks), 3 (discontinuous population switching), and 1 (effective coupling sign change). Of these, the latter occupies the largest area. We will discuss the implications of this findings in the following section.

It should be emphasised that in figure 4 the boundaries between “phases” 1 and 2, and between “phases” 3, 5, and 6 are a matter of convention and do not correspond to sharp transitions of any kind. Rather, they merely mark the changes in mutual locations of transmission peaks *as defined by equation (35)* on one hand, and phase lapse/discontinuity on the other.

When the value of U is reduced to $U < 0.04t$ (while keeping the other QD parameter values in figure 4 constant), the bold line marking the onset of the discontinuity no longer intersects the 1-2 “phase” boundary. In this case, “phases” 5, 6, and 7 disappear and the area of “phase” 1 formally extends down to the $\kappa = 0$ axis at a certain range of values of α . In the $U = 0.03t$ case [see the green lines in figure 6], this range is given by $\alpha_1^{(-)} \approx -0.31 < \alpha < \alpha_2^{(-)} \approx -0.2$ and $\alpha_2^{(+)} \approx 0.18 < \alpha < \alpha_1^{(+)} \approx 0.3$. At this values of α and for small right-left asymmetry $\kappa \ll 1$, the “continuous population switching” scenario as discussed in section 5 *formally* results in an occurrence of the phase lapse between the two transmission peaks [as defined by equation (35)]. We stress however that at least for the moderate values of κ , the entire region, $\alpha_1^{(-)} < \alpha < \alpha_1^{(+)}$ the QD is outside the Coulomb blockade regime (transmission peaks are not well separated, as exemplified by the dashed line in figure 8). As a consequence, equation (35) (used by us to define “phase”1) loses accuracy, making our convention for distinguishing between “phases” 1 and 2 problematic.

We note that the values of $\alpha_1^{(\pm)}$, marking the onset of the discontinuous behaviour, are in a good agreement with equation (52), which at $U = 0.3t$ yields $|\alpha_c| \approx 0.3$. With a further increase of $|\alpha|$ towards $|\alpha| = 1$ the Coulomb blockade effects set in even at $U = 0.3t$.

7. Discussion

Conclusions of the present mean-field study. Anticipated results for a mean-field treatment of multi-level dots. Role of quantum fluctuations: available results and outstanding questions.

Broadly speaking, our mean-field treatment of the interacting two-level dot yields the following result, which holds provided that the interaction is sufficiently strong, see equation (51):

Irrespective of the original sign of the dot-lead coupling, the transmission phase lapse in an interacting QD generally occurs between the two transmission peaks.

There are *two distinct correlation-induced mechanisms* which bring about this uniform situation. Of these, one is related to the off-diagonal (“excitonic”) correlations

on the dot [30] and requires the presence of a finite left-right asymmetry in the original dot-lead coupling (as can be expected generally in the experimental realisations). The other, which in its pure form is operational in the left-right symmetric case, has to do with the correlation-induced “population switching” [15, 17], which can occur either discontinuously (in the Coulomb blockade regime) or continuously (this leads to the Coulomb blockade being lifted).

At the most basic level, the two mechanisms share the same origin, familiar from the standard solid state physics: namely, when a band or an impurity level resides at the chemical potential and is therefore partially filled, energy may be gained by increasing the width of the band or by broadening the impurity level. In case of the “excitonic” mechanism, this “broadening” of the narrower QD level is achieved via a strong increase of hybridisation with the broader level. This in turn is associated with the change of the coupling sign, causing the $-\pi$ phase lapse to occur between the two transmission peaks. In case of the discontinuous population switching [17], the levels of a partially filled dot are abruptly rearranged in such a way that the narrower level never actually crosses the chemical potential. This “jump” of the narrow level (say, E_1) from $E_1 > \mu$ to $E_1 < \mu$ with increasing μ is accompanied by a similar jump of the transmission zero Z and therefore leads to an abrupt change of a transmission phase, $\Delta\Theta_{tr} > -\pi$ (renormalised phase lapse [30]). Continuous population switching in the relevant regime (which arises only for smaller values of U , see sections 5 and 6) involves the two levels approaching the chemical potential at the same time (along with the transmission zero) and is accompanied by a phase lapse of $-\pi$ in the absence of the two well-defined transmission peaks.

The behaviour of a QD for general values of the left-right and 1-2 coupling asymmetries can be understood in terms of *superposition of these two mechanisms*. The continuous population switching scenario can evolve into the “excitonic” one via a smooth crossover with increasing left-right asymmetry. The interplay of these two with the discontinuous population switching mechanism, on the other hand, gives rise to a number of different intermediate “phases”. These are characterised by different numbers (1 or 2) and mutual locations of phase jump(s) and transmission peak(s). Our results suggest that on the whole, the behaviour found in most cases is the one dominated by the “excitonic” mechanism, with a phase lapse of $-\pi$ located between the two well separated Coulomb blockade peaks.

From the theoretical standpoint, our results give rise to the following two questions: (i) how are these findings generalised in the case of a multi-level interacting QD? (ii) What is the role of fluctuations, neglected in our mean-field treatment? We will now address these issues in some detail.

(i) *Multi-level dots within the mean-field approach*. In general, one can expect that *our conclusions will hold for a multilevel dot*, with the two levels nearest the chemical potential playing the role of an “effective” two level QD, which at least at the mean field level would behave in a qualitative agreement with our results. One expected change is that *the parameter area corresponding to the effective sign change (“excitonic”)*

mechanism will be expanded at the expense of the other “phase diagram” regions (dominated in the mean field approach by the population switching). Indeed, for a two-level dot the ineffectiveness of this mechanism in the absence of the right-left asymmetry (section 4) can also be viewed as originating from the fact that each of the dot levels is coupled to a different “subset” of carriers in the lead (odd and even wavefunctions), making the inter-level hybridisation impossible. For a multi-level dot, the number of dot levels exceeds the number of such subsets (which of course remains equal to two, even and odd). Hence even if the two levels adjacent to the chemical potential have different coupling signs and only a small right-left asymmetry, each of these will hybridise with other levels further away (some hybridised combinations may even be decoupled from the leads [34]. This will in turn give rise to a left-right asymmetry of the “effective” two-level QD provided these other levels have asymmetric couplings to the two leads. On the other case, we saw (section 4) that even a moderate amount of initial left-right asymmetry is sufficient to activate the “excitonic” mechanism of the effective coupling sign change.

These conclusions are in a qualitative agreement with the numerical results for multilevel dots [21]. We note, however, that these calculations [21] were performed using the functional renormalisation group method, and therefore include fluctuations at some level.

We also note that within the mean-field approach the *discontinuous evolution* of the QD parameters (driven by the discontinuous population switching mechanism) *will persist within the corresponding range of parameter values also in the case of a multi-level QD*. The physical reason for this is the same as in the two-level case (section 5): suppose that one of the QD levels is fully uncoupled from the leads (and from the other levels). It is then clear that with increasing μ it will eventually be filled in a discontinuous manner (the occupancy jumping from 0 to 1), leading to a discontinuity in all the QD properties [17]. *Within the mean-field treatment*, such a discontinuity originates from a jump between different solutions to the mean field equations, and therefore indicates a presence of a multiple-solution area in the parameter space. This area has a finite size, and therefore removing it altogether and thus eliminating the discontinuity requires a finite (as opposed to infinitesimal) dot-level coupling. Like in the two-level case, the discontinuous evolution will be accompanied by a renormalisation [30] of the corresponding phase lapse values, $\Delta\Theta_{tr} > -\pi$; the conductance at the corresponding values of chemical potential or gate voltage would not vanish. As described in section 6, there will also arise a number of borderline “phases”; in some of these, the additional positive phase jumps would appear.

(ii) *Role of quantum fluctuations* (validity of the mean field approach). The present mean field treatment does not include the effects of fluctuations. It is therefore important to understand to what extent do these alter the overall picture. While considerable effort has been made recently in this direction [20, 21, 22, 23, 24, 25], certain questions still remain unanswered. Below we will attempt to summarise the available results while pointing out the open problems.

First, we note that the available numerical and renormalisation group studies suggest that the *generic effects of electron-electron interaction on the dot include the appearance of the phase lapse between the two transmission peaks*. This is in qualitative agreement with the mean field results. On the other hand, the essentially many-body features like the “resonances” surrounding the transmission zero [20, 21], which originate from the Kondo-type physics [24, 25] *cannot* be reproduced at the mean field level.

Our mean field results suggest the *presence of two distinct correlated mechanisms* causing the phase lapse to occur within the inter-level energy interval. This is in line with recent renormalisation group results [25], suggesting that the QD behaves differently in the right-left symmetric (“parallel effective field” [25]) and asymmetric (“tilted effective field”) cases.

Of the two mechanisms identified within the present mean field approach, the “excitonic” one (involving *off-diagonal correlations on the dot*, section 4), which requires the presence of some right-left asymmetry in the dot-lead coupling ($w_0 \neq 0$), is found to be more generic. Indeed, it gives rise to the prevalent “phase” 1 in our “phase diagram”, figure 4. This mechanism is not related to instabilities of any kind, and can be expected to remain robust beyond the mean field. While this is again in line with the available results, a more qualitative comparison can and should be made in order to confirm that we correctly identified the underlying physics. To this end, one should verify that the off-diagonal average, $\tilde{n}_{12} = \langle \tilde{d}_1^\dagger \tilde{d}_2 \rangle$ indeed shows a sharp peak in the regime of partial QD occupancy [cf. figure 5 (b)]. While the quantity \tilde{n}_{12} should be readily available from numerical calculations, we are not aware of any published results for it⁺. We note that the diagonal average values, $\tilde{n}_{1,2}$, have been calculated recently by the numerical renormalisation group [21] and functional renormalisation group [22] methods, as well as analytically [25]. In the relevant range of values of parameters, their dependence on the gate voltage shows strong non-monotonicity (first noticed in the mean-field studies of the right-left symmetric case [27, 28]) and looks rather similar to the mean field results as seen in figure 5 (b). Another interesting question is related to the degree of 1-2 level coupling asymmetry required for this mechanism to be effective. The corresponding mean-field result, equation (52), differs from the one obtained via the renormalisation group calculation in the “local moment” regime [reference [25], equation (70)] and a systematic numerical investigation is required in order to establish whether (and when) either of these is close to the actual value.

The other mean field mechanism which gives rise to a phase lapse between the Coulomb blockade peaks is that of *discontinuous population switching* (section 5). While the physical origins of the discontinuity are quite clear (see above), the associated notion of multiple solution region is restricted to the mean field approach. Thus, the discontinuous scenario will surely be strongly affected by the fluctuations. At present, it is not clear whether it survives in the exact treatment. Neither the discontinuity, nor

⁺ Our results are in a qualitative agreement with Equation (52) of reference [25] which suggests that \tilde{n}_{12} reaches a maximum in the general area of the point where $\tilde{n}_1 = \tilde{n}_2$. This result [25] should become exact in the large- U , $\tilde{n}_1 + \tilde{n}_2 \rightarrow 1$ limit (“local moment regime” [25]).

the associated “renormalised” phase lapses [30] were found (except at isolated points [22]) in either the functional renormalisation group [21, 22], numerical renormalisation group [21, 22], or analytical renormalisation group/Bethe *ansatz* [24, 25] treatments.

Lastly, we wish to turn to the situation of *perfect right-left symmetry* ($w_0 = 0$) and argue that it *represents a singular case where the effects of fluctuations are most pronounced*. Indeed, owing to the symmetry of this case the hybridisation, \tilde{n}_{12} , and hence the effective intra-dot hopping w remain equal to zero for all values of chemical potential or gate voltage (section 4). Hence the transmission zero, equation (38), remains outside the energy interval between the two transmission peaks at all times (at least in the Coulomb blockade regime, which is of interest to us here). We conclude that within the *mean field approach* for $w_0 = 0$ the only possibility to observe a phase lapse between the two well separated (Coulomb blockade) transmission peaks is via a discontinuous restructuring of the spectrum, as explained in section 5 (figure 7). In this case, the phase lapse is renormalised [30], and is not accompanied by a transmission zero [30, 33].

On the other hand, the numerical results[21], as well as those of the renormalisation group approach [24, 25], reliably indicate that at least for some values of 1-2 asymmetry in the right-left symmetric case, the phase lapse of exactly $-\pi$, associated with a transmission zero, does occur between the two Coulomb blockade peaks. This cannot be reconciled with the mean field picture *at all*, via any sort of renormalisation of the mean field parameters (which could be held responsible for the suppression of discontinuous behaviour at $w_0 \neq 0$). Rather, fluctuations in this case must be giving rise to a totally new physics (albeit perhaps only in the narrow interval of values of chemical potential/gate voltage around the transmission zero). We note that from the point of view of renormalisation group analysis [25] the $w_0 = 0$ (“parallel effective field”) situation does correspond to a special case, and its relationship to behaviour at $w_0 \neq 0$ remains unclear.

Acknowledgments

The authors thank A. Aharony, R. Berkovits, J. von Delft, O. Entin-Wohlman, M. Goldstein, M. Heiblum, V. Kashcheyevs, I. V. Lerner, V. Meden, Y. Oreg, A. Schiller, and H. A. Weidenmüller for enlightening discussions. This work was supported by the ISF (grants No. 193/02-1, No. 63/05, and the Centers of Excellence Program), by the BSF (grants # 2004162 and # 703296), and by the Israeli Ministry of Absorption. YG was also supported by an EPSRC fellowship.

References

- [1] Yacoby A, Heiblum M, Mahalu D and Shtrikman H 1995 *Phys. Rev. Lett.* **74** 4047
- [2] Schuster R, Buks E, Heiblum M, Mahalu D, Umansky V and Shtrikman H 1997 *Nature* **385** 417
- [3] Avinun-Kalish M, Heiblum M, Zarchin O, Mahalu D and Umansky V 2005 *Nature* **436** 529
- [4] Entin-Wohlman O, Hartzstein C and Imry Y 1986 *Phys. Rev. B* **34** 921
- [5] Gefen Y, Imry Y and Azbel’ M Ya 1984 *Phys. Rev. Lett.* **52** 129

- [6] Feldman D E and Gefen Y 2001 unpublished
Gefen Y 2002 *Quantum Interferometry with Electrons: Outstanding Challenges* ed Lerner I V *et al* (Dordrecht: Kluwer) p 13
- [7] Aharony A, Entin-Wohlman O and Imry Y 2003 *Phys. Rev. Lett.* **90** 156802
- [8] Berkovits R, Gefen Y and Entin-Wohlman O 1998 *Phil. Mag. B* **77** 1123
- [9] Oreg Y and Gefen Y 1997 *Phys. Rev.* **B55** 13726
- [10] Silva A, Oreg Y and Gefen Y 2002 *Phys. Rev. B* **66** 195316
- [11] Kim T-S and Hershfield S 2003 *Phys. Rev. B* **67** 235330
- [12] Leturcq R, Graf D, Ihn T, Ensslin K, Driscoll D D and Gossard A C 2004 *Europhys. Lett.* **67** 439
- [13] Weidenmüller H A 2002 *Phys. Rev. B* **65**, 245322
- [14] Taniguchi T and Büttiker M 1999 *Phys. Rev.* **B60** 13814
Levy Yeyati A and Büttiker M 2000 *Phys. Rev. B* **62** 7307
- [15] Hackenbroich G, Heiss W D and Weidenmüller H A 1997 *Phys. Rev. Lett.* **79** 127
Baltin R, Gefen Y, Hackenbroich G and Weidenmüller H A 1999 *Eur. J. Phys. B* **10** 119
- [16] Hackenbroich G, Heiss W D and Weidenmüller H A 1998 *Phil. Mag. B* **77** 1255
- [17] Silvestrov P G and Imry Y 2000 *Phys. Rev. Lett.* **85** 2565
- [18] Berkovits R, von Oppen F and Gefen Y 2005 *Phys. Rev. Lett.* **94** 076802
- [19] Büsser C A, Martins G B, Al-Hassanieh K A, Moreo A and Dagotto E 2004 *Phys. Rev.* **B70** 245303
- [20] Meden V and Marquardt F 2006 *Phys. Rev. Lett.* **96** 146801
- [21] Karrasch G, Hecht T, Oreg Y, von Delft J and Meden V 2006 *Preprint cond-mat/0609191*
- [22] Karrasch G, Hecht T, Weichselbaum A, von Delft J Oreg Y and Meden V 2007 *New J. Phys.* this issue, p. [*Preprint cond-mat/0612490*]
- [23] Kim S and Lee H-W 2006 *Phys. Rev. B* **73** 205319
- [24] Lee H-W and Kim S 2006 *Preprint cond-mat/0610496*
- [25] Kashcheyevs V, Schiller A, Aharony A and Entin-Wohlman O 2007 *Phys. Rev. B* **75** 115313
- [26] Lindemann S, Ihn T, Bieri S, Heinzel T Ensslin K, Hackenbroich G, Maranowski K and Gossard A C 2002 *Phys. Rev. B* **66** 161312
Johnson A C, Marcus C M, Hanson M P and Gossard A C 2004 *Phys. Rev. Lett.* **93** 106803
Kobayashi K, Aikawa H, Sano A, Katsumoto S and Iye Y 2004 *Phys. Rev. B* **70** 035319
- [27] König J and Gefen Y 2005 *Phys. Rev. B* **71** 201308
- [28] Sindel M, Silva A, Oreg Y and von Delft J 2005 *Phys. Rev. B* **72** 125316
- [29] Khomskii D I and Kocharyan A N 1976 *Solid State Commun.* **18** 985
Khomskii D I and Kocharyan A N 1976 *Zh. Expt. Teor. Fiz.* **71** 767 [English translation: 1976 *Sov. Phys. JETP* **44** 404]
- [30] Golosov D I and Gefen Y 2006 *Phys. Rev. B* **74** 205316
- [31] Oreg Y 2007 *New J. Phys.*, this issue, p.
- [32] Baym G and Kadanoff L P 1961 *Phys. Rev.* **124** 287
- [33] Goldstein M and Berkovits R 2007 *New J. Phys.* this issue, p. [*Preprint cond-mat/0610810*]
- [34] Berkovits R., von Oppen F. and Kantelhardt J. W. 2004 *Europhys. Lett.* **68**, 699